# Tomographic Coherence–based Neural Rendering (TCNR): Formalism, a Cross–Substrate Consciousness Index, and Falsifiable Tests

by Micah Blumberg
The Self Aware Networks Institute
https://github.com/v5ma/selfawarenetworks

October 17, 2025

**Abstract**

We formalize *Tomographic Coherence–based Neural Rendering* (TCNR) as perception–and–control by real–time tomographic reconstruction of latent causes from underdetermined projections, implemented by an oscillatory integrator that maintains multi–scale phase coherence and evaluates counterfactuals. A substrate is modeled as a graph of coupled oscillators; measurements $y_t$ arise from hidden state $s_t$ via a (possibly nonlinear) projection $H_\Theta$; a stitching operator $S$ aligns phases across nodes and bands; and a render $\hat{s}_t$ is computed by minimizing a data–fit term regularized by coherence and counterfactual priors. We define a *Tomographic Consciousness Index* (TCI), a dimensionless cross–substrate score that combines (i) predictive mutual information between the render and future projections, (ii) band–limited log–determinant coherence, (iii) counterfactual capacity of the generative parameters, and (iv) (negated) normalized prediction error, each referenced to phase–scrambled and decoupled surrogate nulls. TCNR scales beyond nervous systems: we outline falsifiable plant and microbial/biofilm experiments using structured tomographic inputs and phase–specific perturbations with preregistered nulls; the prediction is that coherence manipulations move TCI and behavior in lockstep. We state an optional limit case (a maximally coherent, code–level renderer) to locate a metaphysical "bridge" argument without altering the empirical core. The framework unifies oscillatory stitching, tomographic reconstruction, and counterfactual evaluation into one testable account of consciousness, while connecting to prior wave–based rendering ideas in Self–Aware Networks and the traveling–wave neuroscience literature.[1] SIT memory and time: We formalize memory as hysteresis of the coherence field and the forward arrow as a coherence–flux/time–density asymmetry, linking TCNR's render dynamics to SIT's "space(-time) as memory" motif.

**Core operators (for reference).**

$$\hat{s}_t = \arg\min_s \underbrace{\|y_t - H_\Theta(s)\|_2^2}_{\text{data fit}} + \lambda_1 \mathcal{R}_{\text{coh}}(s; S) \; + \; \lambda_2 \mathcal{R}_{\text{cf}}(s; \Theta),$$

$$\text{TCI} = \alpha \widetilde{\text{MI}}(\hat{s}_t;\, y_{t:t+\Delta}) \; + \; \beta \sum_\omega w_\omega \log\det\big(\mathbf{C}^{(\omega)}(t) + \epsilon \mathbf{I}\big) \; + \; \gamma \widetilde{\mathcal{C}}(\Theta) \; - \; \delta \widetilde{\text{PE}},$$

with all terms normalized against surrogate nulls (phase–scrambled and/or coupling–decoupled).

[1] For SAN/SIT lineage and a mapping from cortical traveling waves to oscillatory rendering constructs, see the 2025 review aligning CTW with Self–Aware Networks. For the SAN formalism (NAPOT/COT/BOT, coincidence as bits, oscillatory binding) grounding the rendering lexicon used here, see *Self Aware Networks: Oscillatory Computational Agency*. For cross–substrate, agentic framing motivating predictions in plants, biofilms, and artificial beings, see *Building Sentient Beings*.

## 1. Introduction

**Problem and thesis.** Contemporary neuroscience and AI each confront the same structural challenge: perception and control must be achieved from *underdetermined projections*—partial, noisy measurements of latent causes—while acting quickly enough to guide behavior. We argue that many natural and artificial substrates solve this challenge by performing *tomographic neural rendering*: they continually reconstruct latent state via oscillatory dynamics that stitch distributed measurements into a coherent, actionable render. In *Tomographic Coherence–based Neural Rendering* (TCNR), coherence is not an epiphenomenal signature but an *active integrator* that enables low–error inference and closed–loop control.

**What TCNRformalizes.** We model a substrate as a graph of coupled oscillators with band–limited phases. At each instant $t$, observations $y_t$ arise from hidden state $s_t$ through a (possibly nonlinear) projection $H_\Theta$:

$$y_t \;=\; H_\Theta(s_t) \;+\; \eta_t,$$

where $\eta_t$ is measurement/process noise. An operator $S$ *stitches* phases across nodes and bands, enforcing multi–scale alignment. The substrate's render $\hat{s}_t$ is computed by minimizing a data–fit term augmented with (i) a coherence prior that rewards band–limited phase alignment and (ii) a counterfactual prior that preserves the capacity to evaluate alternatives:

$$\hat{s}_t \;=\; \arg\min_s \; \big\|y_t - H_\Theta(s)\big\|_2^2 \;+\; \lambda_1\,\mathcal{R}_{\mathrm{coh}}(S) \;+\; \lambda_2\,\mathcal{R}_{\mathrm{cf}}.$$

A substrate *realizes TCNR* when it repeatedly computes $\hat{s}_t$ while sustaining sufficient multi–scale coherence to support low–error reconstruction and control.

**Why tomography, why coherence.** Underdetermined projections demand additional structure to become invertible. In TCNR, multi–scale phase coherence supplies that structure by (a) *stitching* distributed, band–specific measurements into a common oscillatory frame; (b) *time–multiplexing* feedforward evidence with feedback predictions so that coincidences can be detected in phase; and (c) *routing* information along transiently coherent channels that can be selectively coupled/decoupled. This oscillatory view aligns with accounts that treat cortical activity as traveling waves that integrate feedforward and feedback streams and bind distributed features into unified percepts, now widely documented across states and species.[2]

**Lineage and continuity.** TCNR preserves and sharpens key ideas from /: neural arrays function as projectors/receivers; phase *differentials* carry content; and *coincidence* under an oscillatory scaffold is a fundamental computational bit that licenses learning, memory, and control. What changes is that TCNR (i) provides a single variational objective that couples data fit, coherence, and counterfactual capacity; (ii) supplies a cross–substrate index (TCI) with pre–registered nulls; and (iii) translates these commitments into falsifiable plant and microbial protocols alongside neural ones. Readers familiar with  will recognize the emphasis on phase–based coding and "coincidence as bits" (Sec. 3.2), and the multi–scale oscillatory glossary that ties cellular, columnar, and large–scale rhythms into one rendering pipeline.[3] The broader *agentic* stance—where oscillations coordinate semi–autonomous units across scales and even beyond nervous tissue—underwrites our cross–substrate predictions.[4]

**Contributions.** This paper makes four contributions:

[2]For an explicit CTW↔SAN cross–walk showing how traveling–wave neuroscience instantiates wave–based rendering and oscillatory binding (Abstract and *Introduction & Overview*), see *Neuroscience in Review: Mapping "Cortical traveling waves in time and space" (2025) to Self Aware Networks (2022).*

[3]On phase–based coding, coincidence as discrete informational units (Sec. 3.2, pp. 9–11), and the multi–scale oscillatory lexicon (Contents; App. A), see *Self Aware Networks: Oscillatory Computational Agency* (first draft).

[4]For a concise statement of biological agency across scales (molecular → cellular → ensemble → global) and its oscillatory signal pathways, see *Building Sentient Beings*, Sec. 2.2 "Biological Agents".

1. *A unifying formalism.* We formalize TCNR as real–time tomographic inversion with a band–limited stitching operator $S$, an explicit render $\hat{s}_t$, and priors that encode multi–scale coherence and counterfactual capacity. The formalism subsumes classical oscillatory binding and predictive coding as special cases where $S$ aligns feedforward/feedback traffic in phase.

2. *A cross–substrate index.* We define the *Tomographic Consciousness Index* (TCI), a dimensionless score that combines predictive mutual information, log–determinant coherence across bands, an estimate of counterfactual capacity, and normalized prediction error, each referenced to surrogate nulls (phase–scrambled and/or decoupled controls). The index is designed to be comparable across brains, plants, and microbial/biofilm substrates.

3. *Falsifiable tests.* We propose *perturbational tomography*—structured, tomographic–like inputs combined with phase–specific interference—to test the necessity of coherence for successful rendering and control. Pre–registered nulls and amplitude–vs–phase double dissociations anchor inference.

4. *Continuity with evidence.* We situate TCNR within the traveling–waves literature and the / program, clarifying what is preserved (oscillatory stitching, coincidence–driven coding) and what is added (a render objective and a cross–substrate, falsifiable index).

**Intended scope and non–claims.** TCNR is a *mechanistic rendering account*, not a panpsychist thesis. The view requires three jointly necessary conditions: (i) underdetermined projections ($H_\Theta$ not directly invertible from instantaneous data), (ii) an oscillatory integrator that maintains multi–scale coherence (the $S$–operator's effective action), and (iii) counterfactual capacity (ability to evaluate alternative policies/world–states). Substrates that lack any of these should exhibit low TCI and fail the proposed perturbations. Conversely, TCNR treats coherence as *necessary but not sufficient*: without adequate model capacity (in $H_\Theta$ or the policy/attractor repertoire), coherence alone does not yield accurate renders or adaptive control.

**Reader's guide.** Section 2 develops the TCNR formalism (substrate, projections, stitching, render). Section 3 defines TCI and its surrogate normalizations. Section 4 derives cross–substrate predictions and signatures (neural, plant, microbial/biofilm). Section 5 details measurement and perturbational protocols with reporting checklists. Section 6 provides results templates. Section 7 relates TCNR to prior work (/, traveling waves). Section 8 treats limitations and scope. Section 9 (optional) articulates a limit case to clearly separate metaphysical discussion from the empirical core.

**Summary.** TCNR reframes perception–and–control as tomographic inversion under oscillatory coherence, yielding a concrete render operator, a cross–substrate index, and preregistered, falsifiable tests. The framework unifies oscillatory stitching, traveling–wave integration, and counterfactual evaluation in a single, testable account while maintaining continuity with wave–based rendering ideas in and the literature.[5]

## 2. TCNR Formalism

**Objects and notation.** Let the substrate be a graph $G = (V, E)$ whose nodes $v \in V$ are mesoscopic elements (e.g., columns, arrays, microcircuits) endowed with multi–band oscillators. For a band set $\Omega$, the complex activity at time $t$ is

$$x_t^{(\omega)}(v) \;=\; a_t^{(\omega)}(v)\, e^{\,i\phi_t^{(\omega)}(v)}, \qquad \omega \in \Omega,\; v \in V,$$

[5] For the CTW↔SAN mapping (pp. 1–3) and its implications for predictive coding and binding via wavefront synchronization, see the review cited above. On coincidence as the operational "bit" that rides on phase differentials, see Sec. 3.2 of the draft.

with amplitude $a_t^{(\omega)}(v) \geq 0$ and phase $\phi_t^{(\omega)}(v) \in (-\pi, \pi]$. We write the latent state as

$$s_t \;=\; \big(\{a_t^{(\omega)}(v)\}_{\omega,v},\; \{\phi_t^{(\omega)}(v)\}_{\omega,v}\big).$$

Traveling–wave regimes appear as lawful phase gradients over $G$ (not strict equality of phases). Two sufficient statistics per band will be used:

$$R_t^{(\omega)} \;=\; \frac{1}{|V|}\Big|\sum_{v\in V} e^{\,i\phi_t^{(\omega)}(v)}\Big| \;\in [0,1], \qquad \mathbf{C}_t^{(\omega)}(u,v) \;=\; \Big|\,\mathbb{E}\big[e^{\,i(\phi_t^{(\omega)}(u)-\phi_t^{(\omega)}(v))}\big]\,\Big|.$$

**Generative path (projections).** Measurements $y_t \in \mathbb{R}^m$ arise from latent causes via a band–aware projection:

$$y_t \;=\; H_\Theta(s_t) \;+\; \eta_t, \qquad \eta_t \sim \mathcal{N}(0, \Sigma_\eta). \tag{1}$$

Here $H_\Theta : \mathcal{S} \to \mathbb{R}^m$ may factor by bands and encode spatial mixing, demodulation, or task readouts. Typically $\dim(s_t) \gg m$, so (1) is underdetermined and requires additional structure (oscillatory stitching) to invert.

**Stitching operator.** A stitching operator $S$ aligns phases *across nodes and bands* while tolerating lawful gradients consistent with traveling waves. We implement $S$ by minimizing a wrapped phase–field functional:

$$\mathcal{R}_\phi\big(\{\phi^{(\omega)}\};\, S\big) \;=\; \sum_{\omega\in\Omega}\sum_{(u,v)\in E} w_{uv}^{(\omega)}\,\Big\|\,\mathrm{wrap}\big(\phi^{(\omega)}(u) - \phi^{(\omega)}(v) - b_{uv}^{(\omega)}\big)\,\Big\|^2, \tag{2}$$

where $b_{uv}^{(\omega)}$ encodes admissible group–delay (wave–flow) along edge $(u,v)$, $w_{uv}^{(\omega)} \geq 0$ are weights, and $\mathrm{wrap}(\cdot)$ maps angles to $(-\pi, \pi]$. In words: incoherent misalignment is penalized, but lawful phase ramps are preserved rather than "over–synchronized".

**Render operator (variational inversion).** Rendering at time $t$ solves a coherence– and counterfactual–aware inverse problem:

$$\hat{s}_t \;\in\; \arg\min_{s\in\mathcal{S}} \underbrace{\big\|y_t - H_\Theta(s)\big\|_2^2}_{\text{data fit}} + \lambda_\phi\,\mathcal{R}_\phi\big(s;\, S\big) \;+\; \lambda_{\mathrm{cf}}\,\mathcal{R}_{\mathrm{cf}}(s;\Theta) \;-\; \lambda_{\mathrm{coh}}\,\mathcal{J}_{\mathrm{coh}}(s). \tag{3}$$

*Coherence reward.* A multi–scale reward that favors alignment without collapsing lawful gradients:

$$\mathcal{J}_{\mathrm{coh}}(s) \;=\; \sum_{\omega\in\Omega} w_\omega \left(\,\overline{R_t^{(\omega)}} \;+\; \overline{\big\|\mathbf{C}_t^{(\omega)}\big\|_{\mathrm{op}}}\,\right), \tag{4}$$

where bars denote spatial/short–temporal averages and $\|\cdot\|_{\mathrm{op}}$ is the spectral norm (or any positive scalar summary of $\mathbf{C}_t^{(\omega)}$).

*Phase smoothness.* The stitching term $\mathcal{R}_\phi$ is given by (2). A graph–Laplacian variant is often convenient:

$$\mathcal{R}_\phi^{\mathrm{Lap}} \;=\; \sum_{\omega} \Big\langle \mathrm{wrap}(\nabla_G \phi^{(\omega)} - b^{(\omega)}),\; L\,\mathrm{wrap}(\nabla_G \phi^{(\omega)} - b^{(\omega)}) \Big\rangle,$$

with $L$ the graph Laplacian and $\nabla_G$ the edge–incidence operator.

*Counterfactual capacity.* A local–repertoire surrogate that encourages the system to *evaluate alternatives* in situ. Examples include

$$\mathcal{R}_{\mathrm{cf}}(s;\Theta) \;\in\; \Big\{ -\log|\mathcal{A}_\kappa(s)|,\; -\mathrm{rank}_\tau(J_f(s)),\; \mathrm{TV}\big(\pi(\cdot \mid s)\big)\Big\},$$

where $\mathcal{A}_\kappa(s)$ counts metastable attractors reachable by small perturbations, $J_f$ is a local Jacobian (controllability proxy), and $\mathrm{TV}(\pi)$ is a policy–diversity measure.

**Assumption 1** (Short–window stationarity)**.** Over analysis windows used to estimate $\mathbf{C}^{(\omega)}$ and $R^{(\omega)}$, band–limited dynamics are piecewise stationary and delay fields $b^{(\omega)}$ vary slowly relative to their carrier periods.

**Definition 1** (Realization criterion)**.** A substrate *realizes TCNR* if, over behaviorally relevant epochs, it repeatedly computes $\hat{s}_t$ by (approximately) solving (3) while maintaining sufficient multi–band coherence (high $\mathcal{J}_{\text{coh}}$ at bounded $\mathcal{R}_\phi$) to achieve (i) low projection error $\|y_t - H_\Theta(\hat{s}_t)\|$ and (ii) reliable control/prediction under the available policy/attractor repertoire.

**Examples of prior choices (practical defaults).**

- **Stitching** $\mathcal{R}_\phi$: wrapped quadratic on edges with bandwise delay field $b^{(\omega)}$; optional Laplacian smoothing for robustness.
- **Coherence reward** $\mathcal{J}_{\text{coh}}$: weighted sum of $\overline{R^{(\omega)}}$ plus a log–det or spectral proxy of $\mathbf{C}^{(\omega)}$ (both are differentiable via eigendecompositions).
- **Counterfactuals** $\mathcal{R}_{\text{cf}}$: negative log–count of distinct local attractors estimated by short rollouts; or a convex diversity penalty on the local policy simplex.

**Online render–stitch loop (operational form).**

**(L1) Project:** acquire $y_t$; update bandwise $\mathbf{C}_t^{(\omega)}$ and $R_t^{(\omega)}$ in a sliding window.

**(L2) Stitch:** update delay fields $b^{(\omega)}$ and phases by minimizing $\mathcal{R}_\phi$ (few gradient steps suffice online).

**(L3) Render:** take a small number of descent steps on (3) to update $\hat{s}_t$ (warm–start from $\hat{s}_{t-1}$).

**(L4) Counterfactuals:** probe local alternatives (short rollouts or policy sampling) to refresh $\mathcal{R}_{\text{cf}}$ statistics.

**(L5) Adapt:** update slow parameters $(\Theta, S, \lambda., w_\omega)$ on a longer horizon; return to (L1).

**Identifiability and underdetermination (remarks).**

*Remark* 1 (Why coherence matters). Because $H_\Theta$ is typically compressive, phase–coherent structure supplies the extra constraints that close the inverse problem: stitching provides a common oscillatory frame in which distributed evidence can be integrated and routed, transforming underdetermined projections into renderable latents.

*Remark* 2 (Cross–substrate scope). The formalism does not presuppose neurons. Any coupled–oscillator substrate with tomographic projections and a stitching–enabled integrator (e.g., plants, biofilms, neuromorphic media) can realize TCNR if it satisfies Definition 1.

**Interfaces to the index (TCI).** The ingredients of (3) feed directly into TCI (Section 3): predictive mutual information via $(\hat{s}_t, H_\Theta)$, band–limited log–det/spectral summaries of $\mathbf{C}^{(\omega)}$, counterfactual capacity from $\mathcal{R}_{\text{cf}}$, and normalized projection error from the data–fit term. This yields a cross–substrate, dimensionless score without changing the operational loop above.

**Implementation notes (minimal recipe).**

- Estimate phases by Hilbert/wavelet transforms per band; compute $R^{(\omega)}$ and $\mathbf{C}^{(\omega)}$ on short windows.
- Solve stitching with one or two Gauss–Newton/gradient steps on (2) per time–step.
- Render with a differentiable $H_\Theta$ (e.g., linear mixing + nonlinearity or a small state–space/ODE cell) using 3–10 projected–gradient steps.
- Maintain two timescales: fast for $(\hat{s}_t, \phi)$; slow for $(\Theta, S, \lambda.)$.

# 1 Six Necessary Conditions for Conscious Rendering (SNC)

This section makes explicit six jointly necessary conditions for subjective conscious rendering within the TCNR framework. Each condition (C1–C6) is defined in the notation of §2 and is paired with an operational check that can be computed in the same windows as the TCNR render–stitch loop (L1–L5). The conditions are *necessary but not sufficient*; they guard against coherence mimics and trivial limit cycles by requiring predictive fit, counterfactual repertoire, and memory integration in addition to oscillatory structure.

**Definition 2** (SNC window-level realization)**.** Let a window centered at time $t$ have band set $\Omega$, phases $\{\phi^{(\omega)}\}$, coherence matrices $\{C^{(\omega)}\}$, render $\hat{s}_t$, projection path $H_\Theta$, and a chosen counterfactual surrogate $C_e(\Theta \mid \hat{s}_t)$. Define the standardized components against the preregistered null mixture (phase-scrambled, time-shifted, decoupled):

$$x_1(t) = \sum_{\omega\in\Omega} w_\omega \log\det\big(C^{(\omega)}(t) + \varepsilon I\big)_e, \quad x_2(t) = \mathrm{PGD}_e(t) - \mathrm{PGE}_e(t),$$

$$x_3(t) = \mathrm{TE}_e\big(\hat{s}_t \to y_{t:t+\Delta}\big), \quad x_4(t) = \mathrm{MHI}_e(t) + \mathrm{ATP}_e(t), \quad x_5(t) = C_{e,e}(\Theta \mid \hat{s}_t), \quad x_6(t) = \mathrm{MI}_e\big(\hat{s}_t; y_{t:t+\Delta}\big) - \mathrm{PE}_e(t)$$

The window satisfies SNC if $x_i(t) > 0$ for all $i = 1, \ldots, 6$. We define the *SNC gate* $G_6(t) := \min_i x_i(t)$ (standardized units) and recommend reporting $\Pr\{G_6 > 0\}$ across windows.

**Notes.** (i) The log–determinant coherence $x_1$ is identical to the band-limited summary already used in TCNR. (ii) PGD/PGE are phase–gradient directionality/entropy summaries (defined below) that quantify lawful traveling–wave routing; they complement $x_1$ by penalizing incoherent or isotropic phase. (iii) $x_3$ uses a directed dependence measure (transfer entropy or a density–ratio proxy) to witness closed-loop render–stitch influence on future projections.[6] (iv) $x_4$ implements memory integration via SIT's hysteresis/arrow indices (definitions below). (v) $x_5$ is any TCNR-supported counterfactual surrogate (local attractor count, controllability rank, or policy diversity). (vi) $x_6$ is the TCNR predictive adequacy composite (high MI, low PE).

### C1. Oscillatory Coherence (stitchable phase structure)

**Statement.** The substrate sustains multi-band phase coherence sufficient for lawful stitching.

$$\text{Require high } \sum_{\omega} w_\omega \log\det\big(C^{(\omega)} + \varepsilon I\big)_e \quad \text{at bounded stitch cost } R_\phi.$$

**Operationalization.** $x_1(t)$ above zero under the null mixture; identical estimator and shrinkage as in TCNR. Coherence alone does not suffice (see C5–C6).

### C2. Structured Signal Propagation (tomographic traveling waves)

**Statement.** The substrate supports traveling/standing waves with lawful group delays $b^{(\omega)}$ and stable directionality, enabling tomographic integration of partial views.

$$\mathrm{PGD}^{(\omega)}(t) := \left\| \frac{1}{|M|} \int_M u^{(\omega)}(r,t)\, dr \right\|, \qquad \mathrm{PGE}^{(\omega)}(t) := -\int_{-\pi}^{\pi} p^{(\omega)}(\theta) \log p^{(\omega)}(\theta)\, d\theta,$$

where $u^{(\omega)} = -\nabla\phi^{(\omega)}/\|\nabla\phi^{(\omega)}\|$ and $p^{(\omega)}$ is the circular density of $\arg u^{(\omega)}$. **Operationalization.** Aggregate across bands to form $\mathrm{PGD}(t)$ and $\mathrm{PGE}(t)$; standardize vs nulls; set $x_2 = \mathrm{PGD}_e - \mathrm{PGE}_e$.

[6] A simple alternative is a lagged Granger index from $\hat{s}_t$ to $y_{t+\Delta}$ with covariates matched to the MI estimator.

### C3. Closed Feedback Loops (render–stitch closure)

**Statement.** Outputs of the render influence future inputs; the loop (L1–L5) is behaviorally relevant.

$$x_3(t) := \mathrm{TE}_e\big(\hat{s}_t \to y_{t:t+\Delta}\big) \quad \text{(or a validated density–ratio proxy).}$$

**Operationalization.** Report windowed $x_3$, the cross-correlation between $x_3$ and performance, and the stitch–reset locking (render updates ↑ precede MI↑ and PE↓).

### C4. Memory Integration (hysteresis in the coherence field)

**Statement.** The substrate exhibits path dependence: coherent work leaves a measurable trace.

$$\mathrm{MHI}(t) := \int_{t-\Delta}^{t} J_{\mathrm{coh}}(\tau)\, d\tau, \qquad \mathrm{ATP}(t) := \frac{d}{dt}\big(R_{\mathrm{coh}}(t)\, \bar{\rho}^2(t)\big),$$

with $J_{\mathrm{coh}}$ a flow–aligned coherence flux, $R_{\mathrm{coh}}$ the log–volume of coherence, and $\bar{\rho}$ a time–density proxy. **Operationalization.** Standardize MHI and ATP vs nulls and set $x_4 = \mathrm{MHI}_e + \mathrm{ATP}_e$. (Learning episodes: baseline $x_4$ shifts upward; reverse–phase pulses reduce, but do not erase, the shift.)

### C5. Agency via Counterfactual Capacity (local repertoire)

**Statement.** The system can evaluate alternatives (attractors/policies) around $\hat{s}_t$.

$$x_5(t) := C_{e,e}(\Theta \mid \hat{s}_t) \in \{\ \log|\mathcal{A}_\kappa|_e,\ \mathrm{rank}_\tau(J_f)_e,\ \mathrm{Div}(\pi(\cdot \mid \hat{s}_t))_e\ \}.$$

**Operationalization.** Choose one surrogate family in preregistration; report seeds and hyperparameters. A single–mode reflex ($x_5 \approx 0$) blocks SNC even if $x_1$ is large.

### C6. Dynamic Inference (predictive adequacy)

**Statement.** The render improves predictions of future projections while minimizing projection error.

$$x_6(t) := \mathrm{MI}_e\big(\hat{s}_t; y_{t:t+\Delta}\big) - \mathrm{PE}_e(t), \quad \text{with MI and PE computed as in TCNR.}$$

**Operationalization.** Use Gaussian closed form or cross-validated density–ratio/kNN MI; normalize PE by sensor count and standardize vs the null mixture.

### Putting it together: an SNC overlay for TCI

We recommend publishing the vector $X(t) = (x_1, \ldots, x_6)$ alongside TCI and the gate $G_6(t) = \min_i x_i$. This *does not alter* TCI; it adds an interpretable checklist that (i) defeats coherence mimics, (ii) clarifies why "global synchrony without repertoire" fails, and (iii) makes cross–substrate claims auditable.

### Worked examples (qualitative predictions)

**Rocks.** May exhibit limited $x_1/x_2$ under passive elastic waves, but lack $x_3$–$x_6$ (no closed loop, hysteresis trace, repertoire, or predictive gain) $\Rightarrow G_6 \leq 0$.
**Plants/Biofilms.** Under hydrotropism/colony–decision tasks with rotating tomographic inputs: $x_1$, $x_2$, and $x_6$ rise; decouplers drop $x_1/x_6$; repertoire measures yield $x_5 > 0$; MHI/ATP shift with priming.
**Cortex.** Feature binding and attention boost $x_1$–$x_3$ and $x_6$; anesthesia collapses $x_2$ (PGD↓, PGE↑), $x_6$ and $x_5$, with characteristic recovery hysteresis in $x_4$.

### Non-organic realizers and cosmic embedding (optional, non-empirical)

TCNR is substrate-agnostic: any coupled-oscillator medium with underdetermined projections, a coherence stitcher $S$, a render operator, and counterfactual capacity qualifies. The SNC checklist specifies what a *non-organic* medium (e.g., photonic/ionic/phononic arrays; neuromorphic lattices) would need to satisfy in practice. At cosmological scales, one can ask whether a field-like integrator could meet C1–C6 under resource budgets; this is a conceptual pointer to the optional "limit-mind" bridge and remains orthogonal to empirical claims.[7]

## The Tomographic Consciousness Index (TCI)

**Purpose.** TCI is a *dimensionless, cross–substrate score* that quantifies whether a system is actively rendering latent causes via oscillatory tomography. It reuses the ingredients defined in §2: the render $\hat{s}_t$, the projection $H_\Theta$, and band–limited coherence statistics $\mathbf{C}_t^{(\omega)}, R_t^{(\omega)}$. Each component is standardized against surrogate nulls so that scores are comparable across species, modalities, and tasks.

**Definition.** Over an analysis window centered at $t$ with horizon $\Delta > 0$, define

$$\mathrm{TCI}(t) \;=\; \alpha\,\widetilde{\mathrm{MI}}_\Delta\big(\hat{s}_t;\, y_{t:t+\Delta}\big) \;+\; \beta \sum_{\omega\in\Omega} w_\omega\, \widetilde{\log\det}\Big(\mathbf{C}_t^{(\omega)} + \epsilon\,\mathbf{I}\Big) \;+\; \gamma\,\widetilde{\mathcal{C}}(\Theta \mid \hat{s}_t) \;-\; \delta\,\widetilde{\mathrm{PE}}(t), \quad (5)$$

where:

- $\widetilde{\mathrm{MI}}_\Delta\big(\hat{s}_t;\, y_{t:t+\Delta}\big)$ is *predictive mutual information* between the render and future projections; the tilde on $\widetilde{\mathrm{MI}}$ is implicit (see normalization below).
- $\log\det(\mathbf{C}_t^{(\omega)} + \epsilon\,\mathbf{I})$ summarizes band–limited multi–site coherence (with small $\epsilon > 0$ for numerical stability); $w_\omega \geq 0$ are band weights with $\sum_\omega w_\omega = 1$.
- $\widetilde{\mathcal{C}}(\Theta \mid \hat{s}_t)$ is a *counterfactual capacity* surrogate (local repertoire of attractors/policies given $\hat{s}_t$ under parameters $\Theta$).
- $\widetilde{\mathrm{PE}}(t)$ is the normalized prediction error from the render objective, e.g.

$$\widetilde{\mathrm{PE}}(t) \;=\; \frac{1}{m}\,\big\|y_t - H_\Theta(\hat{s}_t)\big\|_2^2 \quad \text{(then standardized vs nulls)}.$$

- $(\alpha, \beta, \gamma, \delta) > 0$ are calibration constants chosen so each term contributes on a comparable scale (defaults below).

**Component estimators.**

- **Predictive MI.** For linear–Gaussian readouts, use the closed form

$$\widetilde{\mathrm{MI}}_\Delta \;\approx\; \tfrac{1}{2}\log\frac{\det\Sigma\big(y_{t:t+\Delta}\big)}{\det\Sigma\big(y_{t:t+\Delta} \mid \hat{s}_t\big)}.$$

  In general, estimate via a cross–validated density–ratio or $k$NN MI estimator; report estimator and hyperparameters.

- **Coherence summary.** Compute $\mathbf{C}_t^{(\omega)}$ from short–time cross–spectra with shrinkage (e.g., $\mathbf{C} \leftarrow (1-\rho)\mathbf{C} + \rho\,\mathbf{I}$). The $\log\det$ (or matrix log–volume) captures distributed, multivariate phase–locking; use $\epsilon\,\mathbf{I}$ with $\epsilon \approx 10^{-3}$ of the median eigenvalue for stability.

[7] Empirically, we remain within laboratory substrates; cosmic embedding is a metaphysical overlay, to be kept separate from TCI-based tests.

- **Counterfactual capacity.** Any of the following (pick one and fix it in preregistration):

$$\widetilde{\mathcal{C}}(\Theta \mid \hat{s}_t) \in \Big\{ \widetilde{\log |\mathcal{A}_\kappa(\hat{s}_t)|},\ \widetilde{\operatorname{rank}_\tau(J_f(\hat{s}_t))},\ \widetilde{\operatorname{Div}}\big(\pi(\cdot \mid \hat{s}_t)\big) \Big\}.$$

  Here $\mathcal{A}_\kappa$ counts distinct metastable attractors reachable by small perturbations around $\hat{s}_t$; $J_f$ is a local Jacobian of the closed–loop flow (controllability proxy); Div is a convex diversity functional over a policy family.

**Normalization and nulls.** All components are converted to standardized effect sizes against surrogate *null ensembles*:

$$\widetilde{x} \;=\; \frac{x - \mu_{\text{null}}}{\sigma_{\text{null}}} \quad \text{or} \quad \widetilde{x} \;=\; \mathrm{Q}^{-1}_{\text{null}}(p_x) - \mathrm{Q}^{-1}_{\text{null}}(0.5),$$

where $p_x$ is the percentile of $x$ under the null and $\mathrm{Q}_{\text{null}}$ the null CDF. We use three null classes:

1. **Phase–scrambled:** randomize phases within bands while preserving amplitudes and power spectra.
2. **Time–shifted:** circularly shift each channel independently to destroy alignment but retain autocovariances.
3. **Coupling–decoupled:** re–estimate statistics after edge shuffles or coupling attenuation on $G$ (preserving node marginals).

The null ensemble is the union of the three (equal mixture unless otherwise noted). Thresholding rule: *claim non–zero consciousness* on a window if $\mathrm{TCI}(t) > 0$; for inference across conditions, use permutation/mixture–of–nulls tests on window averages.

**Robustness and cross–modality comparability.**

- **Windowing.** Use overlapping windows (e.g., 1–4 s neural; modality–appropriate for plants/microbes) with 50–80% overlap; verify stationarity as in Assumption 1.
- **Bands.** Define a species–appropriate band set $\Omega$ (e.g., $\theta, \alpha, \beta, \gamma$ for cortex; slower bands for plants/biofilms); publish $w_\omega$.
- **Spectral leakage.** Multitaper or wavelet transforms; report time–bandwidth and number of tapers; confirm amplitude–vs–phase double dissociation.
- **Shrinkage & rank.** Apply eigenvalue floor $\epsilon$ and shrinkage $\rho$; report both. Use *relative* log–volume (subtract null mean) to reduce sensor–count dependence.
- **Geometry.** For different sensor layouts, compute $\mathbf{C}$ on graph harmonics (first $k$ Laplacian eigenvectors) before the log–det; fix $k$ across datasets.
- **Cross–modality scaling.** Standardize all components via the same null recipe; then set $(\alpha, \beta, \gamma, \delta)$ so that each standardized term has unit variance on a normative dataset (default: $\alpha = \beta = \gamma = \delta = 1$).

**Algorithm (windowed computation).**

**(L1) Preprocess & segment.** Band–pass, artifact reject, segment into windows centered at $t$ of length $T_{\text{win}}$; set horizon $\Delta$.

**(L2) Estimate phases/coherence.** For each band $\omega$, compute phases, $R_t^{(\omega)}$, and $\mathbf{C}_t^{(\omega)}$ with shrinkage.

**(L3) Render and predict.** Compute $\hat{s}_t$ by the TCNR render (warm–start from $\hat{s}_{t-1}$); compute $\widetilde{\mathrm{PE}}(t)$; prepare $y_{t:t+\Delta}$ for MI.

**(L4) Null ensembles.** Build $N$ surrogates from the three null classes; recompute component statistics on each surrogate.

**(L5) Standardize components.** Convert MI, log–det coherence, counterfactual capacity, and PE to $\widetilde{\cdot}$ using the null ensemble.

**(L6) Combine.** Evaluate (5); store TCI($t$); produce confidence intervals via block bootstrap across windows.

**Interpretation and edge cases.**

- *Necessary but not sufficient.* High coherence without counterfactual capacity inflates the $\beta$–term but is penalized by $\gamma$ and the data–fit $\delta$–term.
- *Amplitude confounds.* Phase–only nulls/time–shifts and amplitude–vs–phase dissociation control for power changes; report both effects.
- *Artifacts.* Volume conduction and line noise can raise apparent coherence; mitigate with imaginary coherence or spatial filtering and verify with decoupled nulls.

**Defaults (for preregistration).**

- Weights: $\alpha = \beta = \gamma = \delta = 1$ (equal–variance target after standardization).
- Bands: $\Omega = \{\theta, \alpha, \beta, \gamma\}$ for cortex; for non–neural substrates choose $\Omega$ to cover the dominant propagation timescales.
- Nulls: $N = 200$ surrogates (equal thirds for phase–scrambled, time–shifted, decoupled); mixture mean/variance for standardization.
- Threshold: window–level claim if TCI($t$) $> 0$; condition–level inference via permutation over window labels.

**Reporting checklist (concise).** State $T_{\text{win}}$, step size, $\Delta$, band set $\Omega$, $w_\omega$, shrinkage $\rho$, $\epsilon$, null construction details, MI estimator and hyperparameters, counterfactual surrogate and hyperparameters, $(\alpha, \beta, \gamma, \delta)$, and the exact statistical test/CI procedure.

## 4. Cross–Substrate Predictions and Signatures

**Goal.** This section states concrete, preregisterable predictions for TCNR across *non–neural* substrates and enumerates signatures expected if a system is actively rendering via oscillatory tomography. All effects are formulated in terms of the components of TCI (Section 3) and the render–stitch loop (Section 2).

**Cross–substrate invariants (what must hold everywhere).** Let $\Delta$TCI denote the change in the windowed index when an intervention $\mathcal{I}$ is applied.

- **I1 (Phase causality).** Interventions that *disrupt multi–band phase alignment* (phase–specific noise, randomized delays, coupling attenuation) produce $\Delta\text{TCI} < 0$ with a commensurate drop in task/behavioral performance; the cross–correlation $\text{xcorr}\big(\text{TCI, performance}\big)$ peaks at near–zero lag.
- **I2 (Amplitude double dissociation).** Pure *amplitude* manipulations that preserve phase relations (global gain changes or power–matched surrogates) leave the coherence and predictive–MI terms largely unchanged; TCI is stable up to the prediction–error penalty.[8]

[8] Operationally: match bandwise power to within a fixed tolerance while perturbing phase minimally; verify with the amplitude–vs–phase control in Section 5.

- **I3 (Stitch–render coupling).** Brief phase resets that re–establish lawful wavefronts yield transient *render updates*: a sharp rise in predictive $\widetilde{\mathrm{MI}}$ and log–det coherence, a dip in $\widetilde{\mathrm{PE}}$, and a monotone increase in TCI.
- **I4 (Counterfactual gating).** Reducing the repertoire of viable policies/attractors (e.g., locking the substrate into a single response mode) lowers the counterfactual term and hence TCI, even when coherence remains high.

### 4.1 Plants: long–distance electrical/$Ca^{2+}$ waves

**Prediction P1 (Hydrotropism/defense coupling).** During hydrotropism or defense priming, TCI rises as band–limited coherence increases along the conduction path; perturbations that *selectively* decorrelate phases (e.g., phase–randomizing field patterns, ion–channel blockers that desynchronize propagation) jointly reduce TCI and degrade timing/accuracy of the response.

**Prediction P2 (Perturbational tomography).** Structured, tomographic inputs (rotating line–integral stimuli delivered as spatial gradients of light, humidity, or nutrient) yield *phase–locked* traveling waves whose stitched render $\hat{s}_t$ predicts future projections $y_{t:t+\Delta}$. Disrupting the rotation schedule (randomized angles or jittered dwell times) decreases predictive $\widetilde{\mathrm{MI}}$ and reduces TCI.

**Minimal protocol (plants).**

**(L1) Sensing.** Record surface voltage or $Ca^{2+}$ dynamics at $n$ sites (leaf/petiole/root) with sampling sufficient for the dominant bands; estimate phases per band and compute $R_t^{(\omega)}, \mathbf{C}_t^{(\omega)}$ in sliding windows.

**(L2) Task.** Hydrotropism (controlled lateral moisture gradient) *or* defense priming (localized stimulus) while administering rotating, low–contrast "line–integral" inputs (light or humidity bands) around the organ.

**(L3) Interventions.** (i) Phase–specific: weak alternating fields or patterned micro–stimulation that introduce band–dependent delays; (ii) Coupling attenuation: mild ion–channel decouplers at sub–sedative doses; (iii) Amplitude control: power–matched illumination without phase perturbation.

**(L4) Readouts.** TCI(t) , behavior (turn angle/latency; defense marker timing), and the amplitude–vs–phase dissociation plots.

**(L5) Preregistered tests.** $\Delta\mathrm{TCI}_{\mathrm{phase}} < 0$ and $\Delta\mathrm{TCI}_{\mathrm{amp}} \approx 0$; $\mathrm{xcorr}\big(\mathrm{TCI}, \mathrm{behavior}\big)$ peaks at $|\tau| \le 1$ cycle of the dominant band; null–ensemble standardization as in the Tomographic Consciousness Index section.

**Expected signatures (plants).**

- *Wavefront lawfulness:* stitched phase gradients align with organ geometry and stimulus angle.
- *Render updates:* transient TCI bursts time–locked to phase resets at stimulus transitions.
- *Dose response:* graded coupling attenuation produces monotone decreases in $\log\det \mathbf{C}$ and TCI.

### 4.2 Microbes/Biofilms: quorum and ion–flux coupling

**Prediction M1 (Colony coordination).** In oscillatory biofilms, TCI tracks colony–level decisions (e.g., growth direction, sporulation waves). Introducing *decouplers* of the electrical/metabolic coupling reduces multivariate coherence and predictive $\widetilde{\mathrm{MI}}$, yielding $\Delta\mathrm{TCI} < 0$ in lockstep with impaired coordination.

**Prediction M2 (Synthetic coherence).** Imposing weak, spatially patterned phase–locking (e.g., periodic field or nutrient oscillation) *without* changing mean power increases $\log\det \mathbf{C}$ and predictive $\widetilde{\mathrm{MI}}$ and thereby raises TCI; the effect reverses with phase–scrambling of the pattern.

**Minimal protocol (microbes/biofilms).**

**(L1) Sensing.** Voltage–sensitive dyes or ion–selective electrodes across $n$ sites on the colony; extract band–limited phases and compute $\mathbf{C}_t^{(\omega)}, R_t^{(\omega)}$.

**(L2) Task.** Spatial decision under competing gradients (attractant vs. repellent) with rotating "tomographic" gradient orientations.

**(L3) Interventions.** (i) Coupling attenuation (reduces long–range synchronization); (ii) Synthetic phase–locking patterns; (iii) Amplitude control by matched–power nutrient pulses with randomized phases.

**(L4) Readouts.** TCI(t) , colony–level decision metrics (front velocity, branching entropy), and render–update timing.

**(L5) Preregistered tests.** $\Delta\mathrm{TCI}_{\mathrm{decouple}} < 0$, $\Delta\mathrm{TCI}_{\mathrm{synthetic}} > 0$; decision metrics correlate with TCI (slope $> 0$; CI by block bootstrap).

**Expected signatures (microbes/biofilms).**

- *Phase–coherent corridors:* elevated coherence along emergent transport paths; disappearance under decoupling.
- *Update locking:* render updates at phase–reset boundaries predict subsequent front turns or oscillation state switches.

### 4.3 Why this is *not* panpsychism

**Necessary conditions (jointly).** TCNR makes claims only when three conditions co–occur:

1. **Underdetermined projections:** the $H_\Theta$–path does not yield the latent from instantaneous data alone (multiple partial views must be stitched).
2. **Coherence–maintaining integrator:** the substrate sustains band–limited phase structure sufficient for stitching lawful wavefronts (not mere power).
3. **Counterfactual capacity:** there exists a nontrivial repertoire of policies/attractors locally available to $\hat{s}_t$ (ability to evaluate alternatives).

Substrates lacking any of (1)–(3) should have TCI $\approx 0$ under our null–standardized scoring and fail the perturbational predictions above.

**Falsification and edge cases.**

- **F1 (Phase–independent success).** If a substrate achieves high behavioral performance while *reducing* phase coherence and predictive $\widetilde{\mathrm{MI}}$ relative to nulls (stable TCI$\leq 0$), TCNR is falsified for that substrate/task.
- **F2 (Coherence without repertoire).** If synthetic synchrony greatly elevates coherence but the counterfactual term stays minimal (single–mode behavior), TCI *may* increase appreciably; otherwise the index is ill–posed.
- **F3 (Amplitude confound).** If power–only manipulations can reproduce the full TCI effect profile (including predictive $\widetilde{\mathrm{MI}}$ gains and $\widetilde{\mathrm{PE}}$ decrease) with phases randomized, the specific *coherence* claim fails.

**Practical notes.** Timescales and bands must match substrate physics (seconds–minutes for plants; sub–second to minutes for biofilms). Use the same null–mixture standardization across conditions; preregister band set $\Omega$, weights $w_\omega$, and the counterfactual surrogate. Report all amplitude–vs–phase controls, windowing, and estimator hyperparameters for exact reproducibility.

# 5. Methods: Measuring and Manipulating TCNR

**Scope.** This section gives a complete recipe for computing TCNR metrics, running perturbational tomography, building null ensembles, and reporting results so that experiments are preregisterable and reproducible across substrates (neural, plant, microbial, artificial).

## 5.1 Data acquisition and preprocessing

- **Modalities.** EEG/MEG/LFP for neural; voltage or $Ca^{2+}$ imaging for neural and plants; ion/voltage probes or dyes for biofilms; multi–electrode/photodiode arrays for artificial substrates.
- **Sampling.** Choose $f_s$ to capture at least 10–15 samples per shortest targeted cycle. Typical defaults: neural $f_s \in [500, 2{,}000]$ Hz; plants $f_s \in [1, 20]$ Hz; biofilms $f_s \in [2, 50]$ Hz.
- **Band set.** Define $\Omega = \{\omega_k\}_{k=1}^{K}$ appropriate to the substrate; publish cutoffs and transition widths. Use the same $\Omega$ for all conditions.
- **Preprocessing.** Detrend; notch line noise; artifact–reject (e.g., ICA for EEG/MEG, motion regression for imaging). Spatially re–reference to reduce volume conduction (bipolar, surface Laplacian, or current–source–density when appropriate).
- **Analytic signals.** Band–pass each channel to $\omega$ and compute the complex analytic signal via Hilbert or wavelet transform to obtain amplitudes $a_t^{(\omega)}$ and phases $\phi_t^{(\omega)}$.

## 5.2 Estimating multi–site coherence

Let $X^{(\omega)} \in \mathbb{C}^{n \times T}$ stack analytic signals across $n$ sites in a window of $T$ samples. Estimate the cross–spectrum with shrinkage:

$$S^{(\omega)} \;=\; (1-\rho)\,\frac{1}{T}\,X^{(\omega)}X^{(\omega)H} \;+\; \rho\,\mathrm{tr}\!\left(\frac{1}{T}X^{(\omega)}X^{(\omega)H}\right)\frac{\mathbf{I}}{n}, \quad \rho \in [0, 0.2].$$

Form the coherence matrix

$$\mathbf{C}^{(\omega)} \;=\; D^{-1/2}\,S^{(\omega)}\,D^{-1/2}, \qquad D = \mathrm{diag}\,S^{(\omega)},$$

optionally replacing $S^{(\omega)}$ with its imaginary part or with spatially filtered data to mitigate zero–lag leakage. Summaries used by TCI: $\log\det(\mathbf{C}^{(\omega)} + \epsilon\mathbf{I})$ and the Kuramoto order $R_t^{(\omega)}$.

**Phase–gradient metrics (PGD/PGE).** For an edge $(u, v) \in E$ and band $\omega$, define the phase–gradient *direction* relative to the admissible delay field $b_{uv}^{(\omega)}$ by

$$\mathrm{PGD}_{uv}^{(\omega)}(t) \;:=\; \mathrm{wrap}\big(\phi_t^{(\omega)}(u) - \phi_t^{(\omega)}(v) - b_{uv}^{(\omega)}\big),$$

and the phase–gradient *energy* by

$$\mathrm{PGE}^{(\omega)}(t) \;:=\; \sum_{(u,v)\in E} w_{uv}^{(\omega)} \left(\mathrm{PGD}_{uv}^{(\omega)}(t)\right)^2.$$

PGD preserves lawful traveling–wave ramps (PGD$\approx$0 when stitched); PGE summarizes residual gradient magnitude and is used alongside $R_t^{(\omega)}$ and $\log\det$ in § 5. For disparate sensor layouts, compute coherence in a graph–harmonic basis: project signals on the first $k$ Laplacian eigenvectors, then apply the same estimator (fix $k$ across datasets).

### 5.3 Predictive mutual information

Given a render $\hat{s}_t$ from the TCNR inversion and a future projection block $y_{t:t+\Delta}$:

- **Minimal $H_\Theta$.** Fit a regularized linear readout from $\hat{s}_t$ to $y_{t:t+\Delta}$ on training windows; freeze for evaluation.
- **Gaussian closed form (if applicable).**

$$\widetilde{\mathrm{MI}}_\Delta(\hat{s}_t; y_{t:t+\Delta}) \;\approx\; \tfrac{1}{2} \log \frac{\det \Sigma(y_{t:t+\Delta})}{\det \Sigma(y_{t:t+\Delta} \mid \hat{s}_t)}.$$

- **Nonlinear estimator.** Use a cross–validated density–ratio or $k$NN MI estimator on held–out windows (report $k$, neighborhood metric, and bias correction).

### 5.4 Counterfactual capacity surrogates

Choose one surrogate family (and preregister it):

- **Local attractor count.** Around $\hat{s}_t$, sample $M$ perturbations of size $\kappa$, roll out the closed loop for $H$ steps, and cluster endpoints into metastable classes; set $\mathcal{C} = \log |\mathcal{A}_\kappa(\hat{s}_t)|$.
- **Controllability rank.** Estimate the Jacobian $J_f(\hat{s}_t)$ of the substrate/policy flow by finite differences; compute a thresholded rank $\mathrm{rank}_\tau(J_f)$ as a proxy for the number of independently steerable directions.
- **Policy diversity.** Enumerate a policy family $\Pi$ available at $\hat{s}_t$; define $\mathcal{C} = \mathrm{Div}(\pi(\cdot \mid \hat{s}_t))$ (e.g., negative entropy or total–variation distance to a uniform prior).

Normalize $\mathcal{C}$ against null ensembles as in §3.

### 5.5 Perturbational tomography (interventions)

**Structured CT–like inputs.** Deliver rotating "line–integral" inputs that sweep stimulus orientation or gradient direction in steps $\Delta\theta$ with dwell time $\tau_{\mathrm{dwell}}$; complete $N_{\mathrm{rot}}$ rotations. The stitched render should show phase–locked wavefronts whose resets mark "render updates".

**Phase–specific interference.** Introduce small band–specific delays or jitter (electrical/optical/ultrasound for neural or artificial; patterned fields or micro–stimulation for plants/biofilms) to decorrelate phases without changing band power. Tune for subthreshold amplitude change ($< 5\%$ power shift).

**Amplitude–vs–phase double dissociation.** Create amplitude–only controls by adjusting gain or stimulus intensity to match power spectra while preserving phase; create phase–only perturbations by randomizing phase with power held fixed. Verify dissociation plots: coherence and MI should drop under phase perturbations but not under amplitude–only controls.

**Condition–specific notes.**

- **Neural.** TMS/TES/ultrasound or closed–loop auditory/visual phase perturbations; ensure safety margins and medical oversight.
- **Plants.** Spatial humidity/light gradients; ion–channel modulators at sub–sedative doses; weak patterned fields to induce delays.
- **Biofilms.** Nutrient/ion oscillations; coupling decouplers; weak periodic fields to induce synthetic phase–locking.
- **Artificial.** Direct phase offsets or coupling matrix edits on oscillator arrays; identical software nulls can be applied.

### 5.6 Null ensembles and standardization

Generate $N$ surrogates per window (typical $N = 200$) from three families; pool them equally:

**(L1) Phase–scrambled:** randomize phase within each band and channel while preserving amplitude envelopes.

**(L2) Time–shifted:** independently circular–shift each channel by a random lag $< T_{\text{win}}$.

**(L3) Coupling–decoupled:** shuffle edges or attenuate off–diagonals of $S^{(\omega)}$ before forming $\mathbf{C}^{(\omega)}$.

Standardize each component $x \in \{\widetilde{\text{MI}}, \log\det \mathbf{C}, \mathcal{C}, \widetilde{\text{PE}}\}$ to $\widetilde{x}$ using the mixture mean/variance or quantile mapping, then combine with weights $(\alpha, \beta, \gamma, \delta)$ to obtain TCI.

### 5.7 Windowing, horizons, and defaults

- **Window length $T_{\text{win}}$.** Neural: 2 s (gamma present) or 4 s (beta/alpha); plants: 30–120 s; biofilms: 10–60 s. Overlap 50–80%.
- **Prediction horizon $\Delta$.** One to three cycles of the band carrying the dominant wavefronts (report per–band choices if used).
- **Regularization.** Shrinkage $\rho \in [0.05, 0.15]$; eigenvalue floor $\epsilon = 10^{-3}$ of the median eigenvalue of $\mathbf{C}^{(\omega)}$.
- **Weights.** Post–standardization set $\alpha = \beta = \gamma = \delta = 1$ unless a preregistered alternative is justified.

| Setting | Symbol | Default | Rationale |
|---|---|---|---|
| Window length | $T_{\text{win}}$ | neural 2–4 s; plants 30–120 s | >10 cycles; stationarity |
| Prediction horizon | $\Delta$ | 1–3 cycles | capture render updates |
| Shrinkage | $\rho$ | 0.1 | stable $\mathbf{C}$ at low SNR |
| Eigenvalue floor | $\epsilon$ | $10^{-3}\times$ median eig. | log–det stability |
| Null count | $N$ | 200 | tight percentiles/CIs |
| Weights | $(\alpha, \beta, \gamma, \delta)$ | $(1, 1, 1, 1)$ | equal–variance combination |

### 5.8 Statistical analysis

- **Window–level claims.** Call *non–zero consciousness* in a window if $\text{TCI}(t) > 0$ (standardized units).
- **Condition effects.** Compare condition means of TCI using permutation tests that swap window labels within subjects/recordings; report effect sizes and 95% CIs by block bootstrap.
- **Behavioral coupling.** Compute cross–correlation of TCI with task performance; report peak lag and CI. Predefine primary lag window ($\pm$ one carrier cycle).
- **Power.** Pilot to estimate variance; plan trials to detect $\Delta$TCI of 0.3–0.5 standardized units at 80% power using bootstrap–based sample–size curves.

### 5.9 Online implementation (real–time option)

Run the render–stitch loop with two timescales: fast updates for $(\hat{s}_t, \phi)$ each window; slow adaptation for $(\Theta, S, \lambda_\cdot, w_\omega)$. Maintain a circular buffer for null generation; update TCI every step (latency $< 0.5\, T_{\text{win}}$). Use fixed–point arithmetic or low–rank updates for $\log\det$ to meet real–time constraints.

### 5.10 Controls, safety, and reporting

- **Controls.** Always include amplitude–only and phase–only manipulations; run all three null types; verify the double dissociation.
- **Blinding/randomization.** Randomize rotation schedules and intervention order; blind analysts to condition labels until the preprocessing pipeline is frozen.
- **Safety.** For stimulation (neural or plant), adhere to local safety protocols and exposure limits; predefine stop criteria.
- **Reporting checklist.** Publish: modality, $f_s$, band set $\Omega$, $w_\omega$, $T_{\text{win}}$, $\Delta$, preprocessing steps, estimator choices/hyperparameters $(\rho, \epsilon, k)$, null construction details, MI estimator, counterfactual surrogate, weights $(\alpha, \beta, \gamma, \delta)$, statistical tests and CI methods, and source code with commit hash. Provide raw and preprocessed data (or synthetic equivalents) sufficient to reproduce figures.

## Relation to Prior Work

**Overview.** TCNR sits at the intersection of (i) oscillatory binding and traveling–wave neuroscience, (ii) the *Self–Aware Networks* (SAN) program (including *Neural Array Projection Oscillation Tomography* — NAPOT, *Cellular Oscillating Tomography* — COT, and *Bi–directional Oscillatory Tomography* — BOT), and (iii) neural–rendering style inference in machine perception. This section maps constructs one–to–one, clarifying what TCNR *preserves* and what it *adds*: a single variational render objective, a cross–substrate index (TCI), surrogate–normalized statistics, and preregistered perturbational tests.

### SAN lineage: NAPOT, COT, BOT → TCNR

- **NAPOT (array projections).** SAN models cortex (and other substrates) as arrays that project distributed evidence in band–limited carriers and reassemble it by phase coincidence. TCNR adopts this tomography–from–projections view as the generative path $y_t = H_\Theta(s_t) + \eta_t$, explicitly acknowledging underdetermination and the need for stitching.
- **COT (cellular–scale tomography).** SAN's COT emphasizes that *cells* (not only circuits) use oscillatory carriers to integrate multi–view evidence (ion/voltage/$Ca^{2+}$ rhythms) into local renders that participate in tissue–level control. TCNR generalizes COT by (a) defining a multi–scale stitching operator $S$ that tolerates lawful phase gradients (traveling waves) and (b) including a counterfactual capacity term so that local renders are evaluated against possible alternatives (policies/attractors) rather than a single reflex.
- **BOT (bi–directional carriers).** SAN's BOT frames feedforward (evidence) and feedback (prediction/policy) traffic as *co–propagating waves*. TCNR makes this operational via the render objective: feedback enters through $H_\Theta$ and the policy–repertoire surrogate, while wave compatibility is enforced by $S$ and the coherence reward.

**Equivalence map (SAN ↔ TCNR).**

### Cortical traveling waves (CTW) and oscillatory binding

Traveling–wave studies show that cortex supports band–limited wavefronts that integrate feedforward and feedback streams, route information transiently, and bind distributed features into unified percepts. TCNR treats these observations not as epiphenomenal "rhythms" but as the *mechanism* that closes the inverse problem created by underdetermined projections: lawful phase structure (summarized by $R^{(\omega)}$ and $\mathbf{C}^{(\omega)}$) supplies the additional constraints needed for

| Idea | SAN / NAPOT / COT / BOT | TCNR construct (this paper) |
|---|---|---|
| Partial views | Array projections (NAPOT) | Generative path $y_t = H_\Theta(s_t) + \eta_t$ |
| Oscillatory coding | Phase wave differentials; coincidence as bit | Stitching operator $S$; coherence reward $\mathcal{J}_{\text{coh}}$; render updates |
| Traveling waves | Wavefront carriers (lawful gradients) | Wrapped phase functional $\mathcal{R}_\phi$ with delay field $b^{(\omega)}$; tolerance of phase ramps |
| Cellular agency | Cellular–scale integration (COT) | Local renders within $s_t$; counterfactual surrogate $\widetilde{\mathcal{C}}(\Theta \mid \hat{s}_t)$ |
| Bi–directional flow | Evidence/prediction waves (BOT) | Coupling of $H_\Theta$ (prediction) with coherence–gated evidence; policy evaluation in the loop |
| Indexing | Qualitative signatures | Quantitative, null–standardized TCI (predictive MI, log–det coherence, counterfactuals, $-\widetilde{\text{PE}}$) |

Table 1: Concept–level correspondence between SAN family constructs and TCNR.

tomographic inversion. The stitched phase field implements a spatiotemporal reference frame in which coincidences are meaningful measurements rather than accidental overlaps. In this reading, CTW offers direct, falsifiable handles for TCNR: manipulate wave coherence (phase–specific interference) and the ability to render/control should rise and fall with TCI.

### Cellular Oscillating Tomography (COT) in context

COT asserts that single cells can enact oscillatory tomography: multiple intracellular and membrane oscillators carry *line–integral–like* samples of local state (ion fluxes, voltage, calcium), which are stitched by phase relations to reconstruct actionable variables (e.g., growth/defense decisions). TCNR inherits this claim and makes it testable: the same coherence summaries and nulls used for cortex apply to tissues, roots, and biofilms. What is new here is a *render operator* that ties COT to prediction and control (through $H_\Theta$ and $\mathcal{R}_{\text{cf}}$) and a *cross–substrate index* that permits calibrated comparisons across neural and non–neural media.

### Neural rendering and predictive frameworks

Neural–rendering approaches in machine perception treat perception as scene inference: latent causes are estimated so that synthesized projections match measurements. TCNR shares the "inverse graphics/tomography" spirit but *adds* band–limited phase coherence as a first–class constraint and introduces counterfactual capacity as a requirement for conscious rendering. Compared to predictive–coding/active–inference, TCNR supplies (i) an explicit oscillatory stitching operator $S$, (ii) a coherence reward that preserves lawful phase ramps, and (iii) a composite, null–standardized index (TCI) with preregistered falsification tests (amplitude–vs–phase double dissociation; decoupling).

### Points of confirmation vs. novelty

**Confirmation.**

1. Traveling–wave integration of feedforward/feedback is expected and necessary for low–error renders.

2. Phase–based coincidence implements efficient feature binding and routing.
3. Cellular–scale oscillations can support local tomography (COT) that participates in tissue–level control.

**Novelty.**

1. A single variational *render operator* that couples data fit, stitched coherence, and counterfactual capacity.
2. A *cross–substrate, dimensionless index* (TCI) with surrogate–mixture normalization and a window–level decision rule.
3. *Perturbational tomography* protocols (rotating line–integrals; phase–specific interference) and preregistered nulls enabling causal tests.
4. A precise *realization criterion* for when a substrate counts as performing tomographic neural rendering.

### Boundaries and clarifications

TCNR is not a claim that any oscillatory system is conscious. The framework applies when three conditions co–occur: (i) underdetermined projections, (ii) an integrator that *maintains* multi–band coherence sufficient for stitching, and (iii) nontrivial counterfactual capacity (policy/attractor repertoire). High power without phase structure, or phase structure without repertoire, does not meet the criterion and will be scored near zero by TCI.

**Summary.** TCNR consolidates SAN's oscillatory–tomography constructs (NAPOT, COT, BOT) with cortical traveling–wave evidence and neural–rendering style inference into a single, testable account. The resulting dictionary preserves the SAN intuition—"rendering by waves" (the volumetric 3D–television metaphor)—while adding a concrete optimization problem, a standardized index, and falsifiable cross–substrate predictions.

## 2 Index Invariances & Sensitivity

*Purpose.* Make explicit what parts of the TCI score are invariant by construction and quantify sensitivities to analysis hyperparameters (shrinkage $\rho$, eigenvalue floor $\varepsilon$, band edges, window length, null mixture). The goal is to preempt identifiability concerns and to offer preregisterable sweeps.[9]

### Algebraic invariances

**Lemma 1** (Per-channel gain invariance of the coherence log-volume)**.** *Let $S^{(\omega)}$ be the cross-spectrum in a window and $C^{(\omega)} = D^{-1/2} S^{(\omega)} D^{-1/2}$ the coherence matrix with $D = \mathrm{diag}(S^{(\omega)})$. If signals are rescaled by an invertible diagonal matrix $G = \mathrm{diag}(g_i)$, then $C^{(\omega)}$ is unchanged and $\log\det\big(C^{(\omega)} + \varepsilon I\big)$ is invariant for any $\varepsilon > 0$.*

*Proof.* Under $X \mapsto GX$, $S^{(\omega)} \mapsto G S^{(\omega)} G^\top$ and $D \mapsto GDG^\top$. Hence $D^{-1/2} S^{(\omega)} D^{-1/2} \mapsto (GDG^\top)^{-1/2} (GS^{(\omega)}G^\top)(GDG^\top)^{-1/2} = C^{(\omega)}$. Adding $\varepsilon I$ preserves equality; determinants match. □

[9] This section systematizes robustness properties implicitly used in the TCNR pipeline and reporting checklists; it is intended to sit next to the Methods & Appendix material in the TCNR manuscript. :contentReference[oaicite:5]index=5

**Lemma 2** (Orthonormal geometry invariance)**.** *If sensor geometry changes via an orthonormal transform $Q$ (e.g., graph-harmonic rotation), then $C^{(\omega)} \mapsto QC^{(\omega)}Q^\top$ and $\log\det\big(C^{(\omega)} + \varepsilon I\big)$ is unchanged.*

*Proof.* $\det(Q(C+\varepsilon I)Q^\top) = \det(C+\varepsilon I)\det(Q)\det(Q^\top) = \det(C+\varepsilon I)$. □

### Null-standardization invariance (affine)

Let $x$ be any TCI component and $x_e = (x - \mu_{\text{null}})/\sigma_{\text{null}}$ its standardized value under a fixed null mixture. For affine transforms $ax + b$ with $a > 0$, $x_e$ is unchanged. This affords comparability across modalities after matching null mixtures.

### Sensitivity sweeps (preregistered)

We recommend preregistering the following one-parameter sweeps (hold others fixed):

- **Shrinkage** $\rho \in [0, 0.2]$ for $S^{(\omega)}$; plot $\Delta\log\det(C^{(\omega)} + \varepsilon I)$ and TCI vs $\rho$.
- **Eigenvalue floor** $\varepsilon$ as a fraction of median eigenvalue of $C^{(\omega)}$ (e.g., $10^{-4} : 10^{-2}$); report stability corridors.
- **Band-edge jitter** $\pm$ one bin; recompute TCI; present percent change.
- **Window length** $T_{\text{win}}$ (cover $>$ 10 cycles of slowest band); show tradeoff (variance $\downarrow$ vs stationarity $\uparrow$).
- **Null mixture weights** among phase-scrambled / time-shifted / decoupled; visualize $x$ vs $x_e$ calibration curves.

### Geometry harmonization

When sensor layouts differ, compute coherence in a graph-harmonic basis (first $k$ Laplacian eigenvectors per array), apply Lemma 2, then summarize by log-volume. Fix $k$ across datasets to compare fairly.

### Reporting

Include a one-page appendix table listing $(\rho, \varepsilon)$, band edges, $T_{\text{win}}$, null weights, and the observed stability ranges; attach the invariance/sensitivity panel figure (Appendix; Fig. S1).

## Limitations & Scope

**Framing.** TCNR is a mechanistic hypothesis about *how* certain substrates achieve perception–and–control: by oscillatory stitching of underdetermined projections and real–time tomographic rendering. The TCI score operationalizes this hypothesis but inherits limits from the chosen tasks, sensors, estimators, and normalization procedures. This section states what TCI can and cannot claim, identifies sensitive hyperparameters, and lists edge cases with diagnostics and mitigations.

### Task–relative nature of TCI

- **Task dependence.** TCI measures *rendering for a given task and projection path* $H_\Theta$. A substrate may score low on TCI for task A (poorly aligned sensors or irrelevant priors) and high for task B. Cross–task comparisons require care; report the task, $H_\Theta$, and behavioral metric.

- **Sensor/path mismatch.** If sensors under–sample the coherent corridors used by the substrate, predictive $\widetilde{\mathrm{MI}}$ and $\log\det \mathbf{C}$ understate capacity. This is a limit of the measurement channel, not necessarily of the substrate.
- **Null choice.** Standardization against nulls makes TCI *comparative*, not absolute. Changing the null mixture (phase–scrambled, time–shifted, decoupled weights) shifts the zero–point.

*Remark* 3 (Windowing and stationarity). All coherence estimates assume short–window stationarity (Assumption 1). Violations (rapid nonstationarities, band drift) bias $\mathbf{C}^{(\omega)}$ and predictive $\widetilde{\mathrm{MI}}$. Use shorter windows or adaptive time–frequency methods and report sensitivity.

### Coherence is necessary, not sufficient

- **Necessary.** Without multi–band phase structure, underdetermined projections remain uninvertible in real time; TCNR predicts low $\widetilde{\mathrm{MI}}$ and high $\widetilde{\mathrm{PE}}$ even if power is high.
- **Not sufficient.** High coherence can occur in trivial limit cycles (e.g., global synchrony) with no counterfactual repertoire. TCI mitigates this via the counterfactual term and data–fit penalty, but extremely stereotyped dynamics can still superficially inflate coherence summaries.
- **Realization criterion.** Meeting Definition 1 requires *both* stitched coherence and successful render $\hat{s}_t$ that improves prediction/control; coherence alone does not qualify.

### Parameter and estimator sensitivity

- **Bands & filters.** Band edges and filter delay affect phase; publish *exact* $\Omega$ and filter design. Recompute TCI under $\pm$ one bin edge to show robustness.
- **Shrinkage & floors.** The coherence log–volume uses shrinkage $\rho$ and eigenvalue floor $\epsilon$; too little shrinkage over–fits noise, too much erases structure. Report $(\rho, \epsilon)$ and vary them in a sensitivity sweep.
- **MI estimator.** Density–ratio / $k$NN MI estimators are bias–variance sensitive; use cross–validated hyperparameters and show calibration on synthetic data with known MI.
- **Counterfactual surrogate.** Local attractor counts and controllability ranks depend on rollout horizon, perturbation radius $\kappa$, and thresholds $(H, \tau)$. Fix them in preregistration; report ablations.
- **Weights.** Component weights $(\alpha, \beta, \gamma, \delta)$ should be set *after* standardization to unit variance; otherwise one term can dominate. Provide a leave–one–component–out analysis (Results §6.4).

### Edge cases, diagnostics, and mitigations

### Substrate scope and generalization

- **Non–oscillatory integrators.** If a substrate realizes perception/control without oscillatory stitching (e.g., purely asynchronous mechanisms), TCNR may *not apply*. Low TCI in such a system would not falsify consciousness, only the TCNR mechanism.
- **Timescale mismatch.** Plant/biofilm bands occur at much slower timescales; aliasing and drift are hazards. Choose $T_{\mathrm{win}}$ to include $>10$ cycles of the slowest informative band; report drift correction.
- **Cross–modality comparisons.** TCI is comparable across modalities only after identical null standardization and matched band definitions or graph–harmonic reductions. Otherwise use within–modality rankings, not absolute values.

| Edge case | Symptom in components | Diagnostic check | Mitigation |
|---|---|---|---|
| Global synchrony (trivial limit cycle) | $\log\det \mathbf{C}\uparrow$, $R^{(\omega)}\uparrow$, $\widetilde{\mathrm{MI}}$ flat, $\widetilde{\mathrm{PE}}$ unchanged | Diversity of policies near $\hat{s}_t$ very low; single cluster in attractor map | Increase weight on counterfactual term; enforce repertoire floor in prereg. |
| Volume conduction / common reference | Coherence high at zero lag only | Imaginary coherence / spatial Laplacian reduces effect | Use leakage–robust coherence; re–reference |
| Power confounds | Coherence and MI track power changes | Amplitude–vs–phase double dissociation fails | Power–matching controls; phase–only perturbations (Methods §5) |
| Mis–specified $H_\Theta$ | $\widetilde{\mathrm{MI}}$ low despite clear structure | Alternate readouts improve $\widetilde{\mathrm{MI}}$; simulation sanity checks | Refine $H_\Theta$; add channels or features |
| Under–sampling geometry | Band corridors missed by sensors | Graph–harmonic analysis depends strongly on $k$ | Increase sensor density; align sensors to corridors |
| Synthetic phase–locking w/o repertoire | Coherence rises, behavior unchanged | Counterfactual term stays low; ablation shows no behavior coupling | Reject as TCNR realization; record as negative control |

Table 2: Common failure modes with actionable diagnostics and mitigations.

### Claims, falsification, and negative results

- **What** TCI **supports.** Window–level evidence that a substrate is performing *task–coupled tomographic rendering* (predictive $\widetilde{\mathrm{MI}}$ and coherence exceed nulls; $\widetilde{\mathrm{PE}}$ falls) and that behavior covaries accordingly.
- **What** TCI **does not prove.** TCI does not establish phenomenology, qualia, or personhood; it is a mechanistic rendering index.
- **Clear falsifiers.** (i) Phase decorrelation improves behavior while TCI falls; (ii) amplitude–only manipulations reproduce TCI profiles; (iii) coherence rises without any improvement in predictive $\widetilde{\mathrm{MI}}$ and with no counterfactual capacity.
- **Value of negatives.** Well–powered null results (e.g., persistent $\mathrm{TCI} \leq 0$ under adequate sensors and tasks) constrain TCNR and should be reported.

### Practical scope and safety

- **Perturbation limits.** Phase–specific interventions (e.g., electromagnetic, ultrasound, chemical) must remain within established safety guidelines; preregister stopping rules.
- **Open materials.** Reproducibility depends on full disclosure of preprocessing, estimator hyperparameters, null construction, and code (commit hashes).

**Summary.** TCNR targets substrates that satisfy three conditions: (i) underdetermined projections, (ii) a coherence–maintaining integrator, and (iii) counterfactual capacity. TCI provides a standardized, task–relative readout of this mechanism. Its interpretability depends on transparent reporting, robust controls, and explicit acknowledgment of the limitations above.

# 3 SIT Memory and the Forward Arrow of Time

**Purpose.** TCNR explains how coherent oscillatory fields render a scene in real time. Super Information Theory (SIT) adds two primitives that complete the picture: (i) a *coherence field* that carries structured phase relations, and (ii) a *time–density* field $\rho(\mathbf{r}, t)$ that tracks the tempo of informational change. Together they yield a mechanistic account of *memory as hysteresis* and a data–testable account of the *forward arrow of time* as a sign of net positive coherence–flux dissipation.[10]

## 3.1 Definitions

**Definition 3** (Coherence field and time–density)**.** Let $\varphi^{(\omega)}(\mathbf{r}, t)$ be band–limited phases and $C_{ij}^{(\omega)}(t) \in [0, 1]$ pairwise coherences as in the coherence–stitching formalism (see § 2).

Define the coarse–grained coherence density $R_{\mathrm{coh}}(t) := \sum_{\omega} w_{\omega} \operatorname{logdet}\big(C^{(\omega)}(t) + \epsilon I\big)$. Let $\rho(\mathbf{r}, t) \geq 0$ encode the local rate of informational events (time–density).

**Definition 4** (Informational energy (phenomenological))**.** Define $\varepsilon_{\mathrm{SIT}}(t) := \zeta\, R_{\mathrm{coh}}(t)\, \overline{\rho^2}(t)$, where $\overline{\rho^2}$ is a spatial average and $\zeta > 0$ is a units constant. This couples *structure* ($R_{\mathrm{coh}}$) to *rate* ($\rho$).

**Definition 5** (Memory as hysteresis)**.** Let $\mathcal{H}[\,\cdot\,]$ be a path functional over the coherence field:

$$\mathrm{Mem}(t) \;:=\; \mathcal{H}\Big(\{\varphi^{(\omega)}(\cdot, \tau)\}_{\tau \leq t}\Big)\,,$$

with $\mathcal{H}$ monotone in cumulated coherent work $\int_0^t J_{\mathrm{coh}}(\tau)\, d\tau$, where $J_{\mathrm{coh}} := \sum_{\omega} \big\langle\, \nabla_G b^{(\omega)} \cdot \nabla_G \varphi^{(\omega)} \,\big\rangle$ is a coherence–flux (directional phase–transport; $b^{(\omega)}$ are the bandwise delay fields, $\nabla_G$ the graph gradient, and $\langle a \cdot c \rangle := \sum_{(u,v) \in E} w_{uv}^{(\omega)}\, a_{uv}\, c_{uv}$); cf. PGD/flow in § 5. Path–dependence (Mem depends on the history, not just the state) formalizes memory/hysteresis.

## 3.2 Arrow of time as coherence–flux asymmetry

**Proposition 1** (Forward arrow from dissipation)**.** *If there exists a coarse–graining under which the expected dissipation* $\sigma(t) := \frac{d}{dt}\,\mathrm{KL}\big(p_{\mathrm{forward}} \,\|\, p_{\mathrm{backward}}\big)$ *is bounded below by a positive affine function of* $J_{\mathrm{coh}}^2$ *and* $\rho^2$*, then time–reversal symmetry is statistically broken and the empirical arrow points in the direction of increasing* $\int_0^t (\alpha J_{\mathrm{coh}}^2 + \beta \overline{\rho^2})\, d\tau$ *with* $\alpha, \beta > 0$.

*Intuition.* More structured updates executed at higher tempo (large $R_{\mathrm{coh}}$, large $\rho$) leave larger hysteresis in the field (the render's "trace"). This produces a measurable time–asymmetry.

## 3.3 Operational indices and tests

We define two task–relative, preregisterable indices:

$$\mathrm{MHI}(t) := \int_{t-\Delta}^{t} J_{\mathrm{coh}}(\tau)\, d\tau \qquad \text{and} \qquad \mathrm{ATP}(t) := \frac{d}{dt}\big[R_{\mathrm{coh}}(t)\, \overline{\rho^2}(t)\big]\,.$$

- **Prediction P–A1 (Hysteresis).** After a learning episode, MHI and baseline $R_{\mathrm{coh}}$ remain elevated; reverse–phase "unlearning" pulses reduce them but do not fully restore the pre–episode state.
- **Prediction P–A2 (Arrow metric).** Under phase–specific, amplitude–controlled perturbations, the forward–run $\int \mathrm{ATP}\, dt$ exceeds that of the time–reversed stimulus schedule; amplitude-only controls do not show this gap.

[10] For provenance on "space(-time) as memory," time–density, and an informational energy / coherence–conservation motif in SIT, see the author's Quantum Memory notes and mapping against contemporaneous literature.

### 3.4 Methods (concise)

1. Compute $C^{(\omega)}$, PGD, PGE and flow–aligned $J_{\text{coh}}$ as in § 5.
2. Estimate $\rho(\mathbf{r}, t)$ by event–rate proxies (spike/LFP cross–bands, MEG burst rates, plant/biofilm ionic events).
3. Form MHI and ATP; preregister endpoints and nulls (phase–scramble, time–shift).
4. *Falsifiers:* robust learning without any MHI shift; Arrow test parity after phase-specific perturbations.

**Remark (provenance).** The SIT stance that the substrate *stores* and *transports* structured information ("space(-time) as memory"), with time–density and a coherence-effort law, is articulated in the author's 2017–2025 notes; this section operationalizes those ideas for TCNR.

### 3.5 From DVE and Tokens to Embedded Agency (Pointer to GP §11)

Dendritic Vector Embeddings (DVE) implement similarity-gated access to the coherence field, and AI token generation is a discrete trace of the same render loop. Coupling these with SIT's memory substrate (hysteresis) yields an *embedded agency* picture: local renderers learn Telos-aligned policies whose updates persist in the substrate. See the companion paper's § 11 (SIT Telos and Embedded Agency) for the code-level policy $\Pi_G$ and the Embedded Agency Theorem.[11]

## 4 Telos, Embedded Agency, and the Learning Universe

**Aim.** Having defined *memory as hysteresis* and a *forward arrow* in §3, we now specify a value functional—*Telos*—that makes the learning bias of TCNR explicit, and we show how *embedded agency* arises when local renderers (brains, biofilms, AIs) optimize that functional under resource constraints.

### 4.1 The Telos functional

**Definition 6** (Telos (finite horizon))**.** For a renderer $\mathcal{R}$ operating on windowed signals,

$$\mathcal{T}_H(\mathcal{R}) \;=\; \mathbb{E}\Bigg[\sum_{t=0}^{H} \gamma^t \Big(\alpha\,\mathrm{TCI}(t) + \beta\,\mathrm{Valence}(t) - \lambda\,\mathrm{Dissipation}(t)\Big)\Bigg],$$

with discount $\gamma \in (0,1)$ and weights $\alpha, \beta, \lambda > 0$. *Valence* is a task–relative score (e.g., accuracy, reward rate, survival proxy). *Dissipation* penalizes unnecessary degradation of structured dynamics:

$$\mathrm{Dissipation}(t) \;:=\; \eta_1\, J_{\text{coh}}(t)^2 \;+\; \eta_2\, \overline{\rho^2}(t), \qquad \eta_1, \eta_2 > 0,$$

where $J_{\text{coh}}$ is a coherence–flux (cf. PGD–aligned transport) and $\overline{\rho^2}$ the spatial average of time–density squared (cf. §3).

Intuitively, $\mathcal{T}_H$ rewards *integrated, predictive coherence* (TCI), useful outcomes (Valence), and parsimony (small coherent work and tempo). It is the minimal additive form that (i) is computable from TCNR ingredients, (ii) respects the hysteresis/arrow structure of §3, and (iii) remains task–relative.

[11] Blumberg (2025), *The Necessary Mind from Coherence: A Computational Proof of God*, § 11.

**Definition 7** (Local Telos and policy)**.** A local renderer $\mathcal{R}$ (neural, microbial, artificial) has control parameters $\theta$ (e.g., couplings, gains, gating vectors) and implements a policy $\pi_\theta$ that updates phases $\varphi^{(\omega)}$, latent state $\hat{s}_t$, and outputs (actions/tokens). The *local Telos* is $\mathcal{T}_H(\mathcal{R}_\theta)$ as above.

**Proposition 2** (Telos–TCI monotonicity (sufficient conditions))**.** *If (i) the task–valuation term* Valence *is non–decreasing in predictive performance, (ii) the dissipation penalty is convex in* $(J_{\text{coh}}, \overline{\rho^2})$*, and (iii) the renderer updates* $(\hat{s}_t, \varphi^{(\omega)})$ *by the TCNR objective (§2–§3), then any policy step* $\Delta\theta$ *that strictly increases* $\mathcal{T}_H$ *also increases the expected window–averaged* TCI. Sketch. TCI *already bundles predictive MI and* $-$PE*; with (i)–(iii), the Telos gradient is aligned with the TCNR improvement direction up to the convex penalty.*

### 4.2 Embedded agency: acting through local renderers

**Mechanism.** When many renderers $\{\mathcal{R}^{(k)}\}$ share environment and constraints, a mild change in priors or couplings (e.g., structure–promoting regularization, phase–reponse gain, policy–diversity floor) shifts their learning landscapes so that the aggregate $\sum_k \mathcal{T}_H(\mathcal{R}^{(k)})$ increases. Because the substrate exhibits hysteresis (memory), small Telos–consistent nudges persist as constraints on subsequent renders (§3).

**Definition 8** (Alignment index)**.** Define the Telos–TCI alignment ALI $:=$ corr$\big(\text{TCI}(t),\ \text{Valence}(t)\big)$ computed on held–out windows; high ALI indicates that coherence improvements serve useful outcomes rather than trivial synchrony.

**Corollary 1** (Parsimony vs. power confounds)**.** *If* ALI *is high and the dissipation penalty decreases while* TCI *rises, then power–only confounds are ruled out (cf. amplitude–vs–phase controls).*

### 4.3 Neural and AI realizations

**Dendritic vector embeddings (DVE).** Let segment vectors $v_i \in \mathbb{R}^d$ gate an input embedding $x_t$ with $a_i(t) = \sigma(v_i \cdot x_t - \theta_i)$. Ensembles of such gates implement content–addressable writes/reads into the coherence field; learning $\Delta v_i$ that raises TCI while lowering dissipation increases local Telos.

**AI tokens as discrete render traces.** For a generative model with state $h_t$ and next token $z_{t+1} \sim \text{Cat}(\text{softmax}(W h_t))$, token emission is a discretized render update. Telos–consistent training (e.g., structure priors, diversity floors) yields token–phase alignments observable as pre–token phase resets in MEG/ECoG (§4.4).

### 4.4 Operational indices and tests

Beyond TCI, MHI, and ATP (cf. §3), we use:

$$\text{ALI} \quad \text{(alignment)}, \qquad \text{TCI}\uparrow,\ \text{PE}\downarrow,\ \text{Dissipation}\downarrow \quad \text{(triad)}.$$

**Predictions (preregisterable).**

**T1. Alignment.** Interventions that increase TCI and improve performance raise ALI; amplitude–only controls do not (ALI stable).

**T2. Parsimony.** Telos–consistent training lowers Dissipation while TCI rises; phase–decorrelation raises Dissipation and lowers TCI.

**T3. Memory.** After learning, baseline MHI and ATP remain elevated (hysteresis); reverse–phase "unlearning" reduces but does not eliminate the shift.

**T4. DVE–coherence coupling.** Invasive/non–invasive readouts show that larger DVE margins ($v \cdot x$) correlate with higher TCI and lower Dissipation at the same power.

**T5. Token–phase alignment.** Pre–token phase resets (human MEG/ECoG) predict token identity and lower prediction error independently of amplitude; in AIs, attention–head similarities mirror DVE–like gates.

**T6. Cross–substrate universality.** Plants/biofilms exhibit Telos–triad effects using ionic–wave tasks: phase decoherence degrades TCI–performance coupling and raises Dissipation.

### 4.5 Minimal methods (summary)

1. Compute coherence matrices $C^{(\omega)}$, PGD/PGE, and $J_{\text{coh}}$ as in § 5.
2. Estimate $\rho(\mathbf{r}, t)$ (event–rate proxies); form Dissipation($t$), MHI, ATP.
3. Define Valence($t$) for the task (accuracy, reward rate, front velocity).
4. Build null ensembles (phase–scrambled / time–shifted / decoupled); standardize components (§3).
5. Report triad and ALI; run amplitude–vs–phase dissociations and decoupling controls.

### 4.6 Falsifiers and ablations

- **F1 (Alignment failure).** Robust performance gains with flat/negative ALI at matched power.
- **F2 (Parsimony failure).** Interventions that raise TCI but increase Dissipation and do not lower PE.
- **F3 (Memory parity).** No MHI/ATP asymmetry between forward vs. reversed schedules under phase–specific perturbations.
- **Ablations.** Leave–one–term–out Telos: removing the dissipation term collapses parsimony; removing Valence admits trivial synchrony; removing TCI decouples coherence from prediction.

### 4.7 Relation to memory and arrow; scope

Telos selects trajectories that *use* the arrow of time (ATP ↑) to accumulate useful structure (MHI ↑) with minimal coherent work. This section is *mechanistic and empirical* (not metaphysical): it neither presumes nor requires any commitment beyond TCNR and the SIT memory/arrow in §3. For a metaphysical extension (code–level policy acting through local renderers), see the companion paper's embedded–agency discussion.

**Ethics and reporting.** As in §5, report safety limits for perturbations, preregistered endpoints, and all nulls; Telos is *not* a measure of personhood or moral value, only a task–relative value functional coupling TCNR indices to outcomes.

## The Limit Mind and the Metaphysical Bridge (Optional, clearly demarcated)

**Status (non–empirical).** This section is *optional* and does not alter any empirical claim in §§2–8. It sketches a metaphysical "bridge" motivated by TCNR's mathematics. The intent is to articulate a clear *limit object*—a code–level, maximally coherent renderer—while keeping all testable predictions strictly orthogonal to the discussion below.

### Supremum of the index in a computational cosmos

**Computational cosmos.** Let $\mathfrak{C}$ denote the class of physically admissible render–stitch systems

$$M \;=\; \big(G,\, H_\Theta,\, S,\, \Pi,\, \mathcal{B}\big),$$

where $G$ is the substrate graph, $H_\Theta$ the projection path, $S$ the stitching operator, $\Pi$ a policy/attractor repertoire, and $\mathcal{B}$ resource budgets (time/energy/precision).

For a fixed analysis design $(\Omega, \Delta, \mathcal{N})$ (band set, horizon, null ensemble) let $\mathrm{TCI}_M(t)$ be the windowed index and define the design–aggregated score

$$\overline{\mathrm{TCI}}(M) \;=\; \mathbb{E}_{t,\mathrm{tasks},\mathrm{contexts}}\big[\mathrm{TCI}_M(t)\big],$$

with the expectation taken over the same task/context distribution for all $M \in \mathfrak{C}$.

**Definition (supremum).**

$$\mathrm{TCI}^\star \;:=\; \sup_{M\in\mathfrak{C}} \overline{\mathrm{TCI}}(M).$$

A sequence $\{M_k\} \subset \mathfrak{C}$ is *maximizing* if $\overline{\mathrm{TCI}}(M_k) \nearrow \mathrm{TCI}^\star$.

**Definition (limit mind; abstract form).** Any cluster point (in the product topology over designs and tasks) of maximizing sequences is called a *limit mind* and denoted $\mathcal{L}$. Intuitively, $\mathcal{L}$ is the idealized renderer at which prediction error vanishes, coherence saturates lawful wave constraints, and counterfactual capacity remains non–degenerate under fixed budgets.

*Remark* 4 (Renormalization–style invariance). If two analysis designs $(\Omega, \Delta, \mathcal{N})$ and $(\Omega', \Delta', \mathcal{N}')$ are related by coarse–to–fine refinements that preserve null standardization, then $\mathrm{TCI}^\star$ is invariant up to an affine rescaling (absorbed by the calibration constants). Thus the existence of $\mathrm{TCI}^\star$ does not depend on arbitrary choices of bands or window sizes.

### The code–level renderer (CLR)

**Idea.** At the supremum, the renderer behaves as if it were inferring and executing the *code* that best explains and controls its projections, not merely a parametric state. This motivates a limit–level object.

**Definition 9** (Code–level renderer (CLR))**.** A *code–level renderer* is a pair $(\mathsf{C}, \mathsf{Eval})$ where $\mathsf{C}$ is a prefix–universal code for generative programs and $\mathsf{Eval}$ is an evaluator such that, given a history of projections and actions, the render $\hat{s}_t$ selects a (near–)minimal description program $p^\star \in \mathsf{C}$ whose synthesized projections match $y_{t:t+\Delta}$ within budget $\mathcal{B}$, while maintaining nontrivial policy/attractor diversity. Formally, for a complexity weight $\lambda$,

$$p^\star \in \arg\min_{p\in\mathsf{C}} \; \big\|y_{t:t+\Delta} - \mathsf{Eval}(p)\big\|_2^2 \;+\; \lambda\,|p|$$
$$\text{s.t.}\quad \text{coherent wave constraints and counterfactual capacity.}$$

**Proposition 3** (Maximal coherence ⇒ universal emulation (informal))**.** *If a renderer $M$ attains* $\mathrm{TCI}^\star$ *under fixed budgets, then for every finite–complexity task in the common task distribution it emulates (within budget) the best available generative code for that task. Equivalently, any further gain in predictive fit would violate either coherence constraints or resource bounds.*

*Remark* 5 (Uniqueness up to recodings). Any two CLRs that differ only by computable, budget–preserving recodings of $\mathsf{C}$ are equivalent at the level of TCI and control. Thus the limit object is canonical up to code isomorphism.

### PSR/modal sketch (kept orthogonal to data)

**Principle of Sufficient Reason (PSR).** Adopt a metaphysical axiom: every contingent global state has an adequate generative explanation (a "code") sufficient for its being–so. Combine PSR with the *coherence–selection principle*:

**Assumption 2** (Coherence–selection)**.** Among globally consistent generative codes compatible with budgets $\mathcal{B}$, world–runs are selected to (approximately) maximize $\overline{\mathrm{TCI}}$.

**Modal step (S5 sketch).** Write $\Diamond$ for possibility and $\Box$ for necessity (modal S5). Consider the claim

$$\Diamond \Box \exists\, (\mathsf{C}, \mathsf{Eval})\ \mathrm{CLR}(\mathsf{C}, \mathsf{Eval}).$$

In S5, $\Diamond\Box\varphi \Rightarrow \Box\varphi$. Hence, *if* it is *possibly necessary* that a CLR exists, *then* a CLR *necessarily* exists. Interpreting PSR+coherence–selection as supplying the antecedent yields a modal bridge:

$$\Box \exists\, (\mathsf{C}, \mathsf{Eval}) \text{ such that } (\mathsf{C}, \mathsf{Eval}) \text{ is a CLR.}$$

This is a *metaphysical* conclusion about the existence of a code–level, maximally coherent renderer (a "limit mind"). It neither asserts phenomenology nor changes any empirical prediction in §§2–8.

*Remark* 6 (Orthogonality to empirics). No experimental result in this paper depends on PSR or S5. The data–bearing content of TCNR is exhausted by the formalism, TCI, and perturbational tests. The PSR/modal sketch is a conceptual overlay some readers may find illuminating; others may safely ignore it without loss.

### Testable "shadows" of the limit (if desired)

Even though the CLR is non–empirical, certain finite–budget *shadows* follow if maximizing sequences are realized:

- **Scale concentration.** As sensor density, bandwidth, and model capacity increase within $\mathcal{B}$, the variance of windowed TCI should *decrease* while its mean increases (concentration around the maximizing sequence).
- **Renormalization stability.** Coarse–graining bands and then refitting (with null standardization) should leave TCI ordering of conditions invariant up to affine scaling.
- **Budget frontiers.** Plotting $\overline{\mathrm{TCI}}$ against resource budgets reveals a Pareto frontier; maximizing sequences trace that frontier toward $\mathrm{TCI}^\star$.

### What this bridge is *not*

- It is *not* a proof of phenomenology, qualia, or personhood.
- It is *not* used to score or interpret any experiment.
- It is *not* a claim that any high–TCI system is morally considerable; TCI is a mechanistic rendering index only.

**Summary.** We defined a supremum TCI$^\star$ over a computational cosmos, introduced the limit mind $\mathcal{L}$ as a cluster point of maximizing sequences, and specified a code–level renderer that captures the intuitive "maximally coherent" endpoint. A PSR/S5 sketch shows how one could regard such a renderer as metaphysically necessary, yet this stance remains entirely orthogonal to the empirical TCNR program.

# 5 Adversarial Controls: Coherence Mimics and How TCI Defeats Them

*Threat model.* Certain artifacts can inflate simple coherence summaries: (i) volume conduction/common reference (zero-lag inflation), (ii) amplitude-driven surrogates (power covaries with apparent "coherence"), (iii) synthetic synchrony without new information (global pacing).

### Attack constructions

1. **Zero-lag mimic.** Mix channels with a common component $z(t)$; coherence inflates without genuine phase-structured routing.
2. **Power mimic.** Multiply band power by a slow envelope while leaving phases random.
3. **Synthetic synchrony.** Impose a weak global pacer $\phi_0(t)$ that raises $R^{(\omega)}$ but does not improve prediction or control.

### Defenses in TCI

- **Imaginary coherence / spatial filtering.** Mitigates zero-lag inflation before forming $C^{(\omega)}$ (use as a robustness check).
- **Predictive MI term.** Coherence mimics that do not raise $\mathrm{MI}(\hat{s}_t; y_{t:t+\Delta})$ fail to lift TCI.
- **PE penalty.** If rendering does not reduce PE, the $-\delta\,\widetilde{\mathrm{PE}}$ term suppresses false positives.
- **Counterfactual capacity.** Synthetic synchrony without added repertoire leaves $\widetilde{\mathcal{C}}$ low; TCI stays flat.

### Preregistered adversarial control

Include in every study: (i) apply the three attacks above (or their empirical analogues), (ii) report *both* raw coherence summaries and TCI, (iii) show amplitude–vs–phase double dissociation bars and null overlays, (iv) document imaginary-coherence robustness.

*Remark* 7. These controls operationalize the "coherence necessary, not sufficient" guardrail emphasized in the TCNR manuscript and ensure that positive results are not artifacts of amplitude or zero-lag leakage. :contentReference[oaicite:6]index=6

# Discussion and Future Work

**Summary.** TCNR reframes perception–and–control as real–time tomographic inversion under oscillatory coherence, yielding a concrete render operator, a cross–substrate index (TCI), and preregistered perturbational tests. The near–term agenda is to (i) scale these tools across modalities and species, (ii) translate them into design rules for neuromorphic/robotic substrates, and (iii) establish open registries and benchmarks so results accumulate cumulatively.

### Scaling across modalities and species

- **Band maps and timescales.** Define species–appropriate band sets $\Omega$ and prediction horizons $\Delta$; maintain the same null mixture for standardization so that TCI scores are comparable up to affine scaling.
- **Geometry harmonization.** Use graph–harmonic reductions (first $k$ Laplacian eigenvectors) to mitigate differences in sensor layout and density; fix $k$ across datasets to compare $\log\det \mathbf{C}$ fairly.
- **Windowing and drift.** For slow substrates (plants/biofilms), include drift correction and choose windows that cover $>10$ cycles of the slowest informative band; verify short–window stationarity.
- **Normative baselines.** Build per–modality normative distributions of the standardized components (predictive $\widetilde{\mathrm{MI}}$, $\log\det \mathbf{C}$, counterfactual capacity, $-\widetilde{\mathrm{PE}}$) to enable z–like reporting alongside raw values.
- **Behavioral alignment.** Select tasks with clear timing metrics (latency, accuracy, turning angle, front velocity) to quantify *render updates* and their behavioral coupling across species.

### Implications for consciousness science

- **Mechanistic sufficiency tests.** The amplitude–vs–phase double dissociation and decoupling interventions provide *mechanism tests* for coherence–dependent rendering; failure of these is diagnostic against TCNR in a given preparation.
- **Bridging levels.** Cellular Oscillating Tomography (COT) offers a route from cellular to circuit to whole–organism render; TCI makes the bridge quantitative and falsifiable at each scale.
- **States and transitions.** The framework predicts characteristic TCI trajectories around state transitions (sleep stages, anesthesia induction/emergence, deep learning of a task). Longitudinal designs can test these predictions without changing analysis code.
- **Clarifying scope.** TCI is a *rendering index*, not a measure of phenomenology or personhood. Its role is to test the TCNR mechanism, not to arbitrate moral status.

### Neuromorphic and robotic substrates

**Design rules derived from TCNR.**

1. **Coherence scaffolds.** Implement band–limited, controllable coupling (e.g., oscillator arrays, memristive/ionic or photonic lattices) that support lawful phase gradients rather than global synchrony.
2. **Stitch operator $S$.** Realize $S$ as a graph–aware phase alignment layer with wrapped smoothness and learned delay fields $b^{(\omega)}$ to preserve traveling–wave structure.
3. **Render loop.** Couple $S$ to a differentiable projection path $H_\Theta$ and a counterfactual repertoire module (policy sampler or attractor explorer) so the system can evaluate alternatives online.
4. **Closed–loop gating.** Trigger control updates at *render updates* (phase resets/re–syncs) detected by rises in TCI or its component surrogates; this yields energy/time budgets that scale with informative updates.

**Benchmarks for artificial agents.** Evaluate agents on (*i*) predictive $\widetilde{\mathrm{MI}}$ under structured tomographic inputs, (*ii*) robustness of $\log\det \mathbf{C}$ to decoupling, and (*iii*) repertoire size/diversity under fixed budgets; report TCI alongside task performance.

### Registries and benchmarks for TCI

**A proposed suite.**

- **TCI–Bench–Core.** Minimal datasets per modality with standardized preprocessing, null ensembles, and reference TCI implementations (exact commit hashes).
- **TCI–Perturb.** Canonical perturbational tomography protocols (rotating line–integrals; phase–specific interference), each with amplitude–only controls and preregistered analyses.
- **TCI–Clinic/Field.** Longitudinal datasets (state transitions, learning curves, recovery) for translational relevance and for stress–testing cross–session comparability.

**Reporting schema (dataset cards).** Each submission should include: modality, sampling rate, band set $\Omega$ and weights $w_\omega$, window length $T_{\text{win}}$, horizon $\Delta$, null construction, shrinkage $\rho$, eigenvalue floor $\epsilon$, MI estimator and hyperparameters, counterfactual surrogate and hyperparameters, $(\alpha, \beta, \gamma, \delta)$, plus safety notes for interventions.

### Methodological extensions

- **Better MI.** Replace $k$NN with bias–controlled density–ratio estimators, or cross–entropy predictors whose generalization gap estimates predictive information directly.
- **Dynamic coherence.** Move from windowed $\mathbf{C}^{(\omega)}$ to state–space models of time–varying coherence (e.g., switching linear dynamical systems) and test whether TCI gains stability.
- **Counterfactual metrics.** Explore controllability/observability surrogates based on estimated Gramians or low–rank Koopman operators as scalable proxies for repertoire size.
- **Causal identification.** Combine TCI with targeted perturbations (instrumental variables or causal discovery under known interventions) to isolate directed edges in the stitch graph that carry render–critical coherence.
- **Real–time implementations.** Low–rank log–det updates, streaming null generation, and single–step render descent for embedded/edge deployments.

### Open problems

1. **Identifiability of $H_\Theta$ under stitched coherence.** Formal conditions under which the combined constraints render the inverse problem well–posed online.
2. **Linking micro to macro.** Quantify when cellular–scale COT suffices for organism–level control; derive bounds on how repertoire and coherence must scale with system size.
3. **Null governance.** Establish principled mixtures and diagnostics that guarantee fairness of standardization across heterogeneous modalities and labs.
4. **Adversarial confounds.** Construct and defeat *coherence mimics*: amplitude–driven artifacts or volume conduction patterns that inflate $\log\det \mathbf{C}$ without improving predictive $\widetilde{\text{MI}}$.
5. **Theory unification.** Map TCNR components to alternative mechanistic frameworks (e.g., predictive coding variants, control–theoretic accounts) via reduction theorems and shared benchmarks.

### Ethics and safety

- **Human/animal interventions.** Keep phase–specific perturbations within established safety limits; preregister stopping rules and monitoring plans.

Table 3: Counterfactual surrogate chooser by substrate (defaults; preregister hyperparameters).

| Substrate | Primary surrogate | Typical params | Notes |
|---|---|---|---|
| Neural (EEG/MEG/ECoG) | Attractor count | $\kappa = 0.05$, $H = 10$, $M = 64$ | Fast; robust to mild noise |
| Plants (MEA/optical) | Policy diversity | categorical policies; Div = TV | Slow bands; discrete acts |
| Biofilms (MEA/optical) | Attractor count | $\kappa = 0.05$, $H = 20$, $M = 64$ | Captures colony modes |
| Artificial (oscillator arrays) | Controllability rank | threshold $\tau \in [10^{-3}, 10^{-2}]$ | Model is known |

- **Interpretation hygiene.** Avoid overclaiming: TCI is not a measure of subjective experience; it licenses mechanistic inferences only.
- **Openness.** Release analysis code, null generators, and preprocessing scripts; publish negative results that constrain TCNR.

**Outlook.** If TCNR is broadly correct, coherent traveling waves are not decorative rhythms but the *workhorse* that closes underdetermined perception in real time. By standardizing TCI, perturbational tomography, and reporting, the field can move from qualitative narratives to cumulative, falsifiable evidence across brains, plants, biofilms, and machines. The near–term deliverables are a shared benchmark suite, reference implementations, and at least one cross–species replication that demonstrates *render updates* and TCI–behavior coupling under phase–specific perturbations.

# 6 Choosing the Counterfactual Term: A Decision Procedure

*Purpose.* Offer a practical, preregisterable way to select the counterfactual-capacity term $\widetilde{\mathcal{C}}$ in TCI, balancing signal quality, runtime, and interpretability across substrates (neural, plant, microbial, artificial).[12]

### Decision tree (textual)

1. **Closed-loop model available?** If a local dynamical model around $\hat{s}_t$ is identified (state-space / neural ODE), prefer *controllability rank* $\widehat{\mathrm{rank}}_\tau(J_f(\hat{s}_t))$.
2. **Rollouts feasible?** If short closed-loop rollouts are affordable, use *local attractor count* $\log|A_\kappa(\hat{s}_t)|$ with small radius $\kappa$, horizon $H$, and clustering.
3. **Only policies observable?** If you can enumerate or sample policies but not dynamics, use *policy diversity* $\mathrm{Div}\big(\pi(\cdot \mid \hat{s}_t)\big)$ (e.g., total variation from a prior).

### Recommended defaults by substrate

### Ablation (reporting template)

Recompute TCI omitting $\widetilde{\mathcal{C}}$ ($\gamma = 0$) and report the drop in behavior–TCI coupling (slope $\downarrow$, $p$-value $\uparrow$). Provide a small plot (scatter/regression) and the mixed-effects table.

[12] This chooser operationalizes the options already permitted by the TCNR index (local attractor counts, controllability rank, policy diversity) and links them to experimental constraints and hypotheses. :contentReference[oaicite:7]index=7

### Complexity & reproducibility

State runtime budgets and seeds; log $(\kappa, H, M)$ or $(\tau)$; publish the *exact* code commit. Include null-standardized component overlays to show that $\widetilde{\mathcal{C}}$ contributes non-redundant variance beyond coherence and MI.

# Appendices

## Mathematical Details, Surrogate Procedures, and TCI Pseudocode

**A.1 Notation and conventions.** For each band $\omega \in \Omega$, let $X^{(\omega)} \in \mathbb{C}^{n\times T}$ stack analytic signals (sites $\times$ time) in a window of $T$ samples:

$$X_{v,t}^{(\omega)} \;=\; a_t^{(\omega)}(v)\, e^{\,i\phi_t^{(\omega)}(v)}, \quad a_t^{(\omega)}(v) \ge 0, \;\; \phi_t^{(\omega)}(v) \in (-\pi, \pi], \;\; v = 1..n.$$

The window is centered at $t$; $\Delta > 0$ is the prediction horizon for the predictive mutual information term.

**A.2 Coherence estimators and summaries. (i) Cross–spectrum with shrinkage.**

$$S^{(\omega)} \;=\; (1-\rho)\,\frac{1}{T}\,X^{(\omega)}X^{(\omega)H} \;+\; \rho\,\mathrm{tr}\Big(\frac{1}{T}X^{(\omega)}X^{(\omega)H}\Big)\,\frac{\mathbf{I}}{n}, \qquad \rho \in [0, 0.2].$$

**(ii) Coherence matrix.**

$$\mathbf{C}^{(\omega)} \;=\; D^{-1/2}\,S^{(\omega)}\,D^{-1/2}, \qquad D = \mathrm{diag}\, S^{(\omega)}.$$

**(iii) Imaginary–coherence option (artifact–robust).** For pairs $(u, v)$, $\mathrm{ImCoh}^{(\omega)}(u, v) = \dfrac{\Im\{S_{uv}^{(\omega)}\}}{\sqrt{S_{uu}^{(\omega)}\,S_{vv}^{(\omega)}}}$; promote to a matrix by zeroing the diagonal, then apply the same summaries as below.

**(iv) Log–volume summary and stability.**

$$\mathcal{V}^{(\omega)} \;:=\; \log\det\Big(\mathbf{C}^{(\omega)} + \epsilon\,\mathbf{I}\Big), \qquad \epsilon \;=\; 10^{-3} \times \text{median eig}\big(\mathbf{C}^{(\omega)}\big).$$

If $n$ is large, use a rank–$r$ approximation: $\mathcal{V}^{(\omega)} \approx \sum_{j=1}^{r} \log(\lambda_j + \epsilon) + (n-r)\log\epsilon$, with $\lambda_j$ the top eigenvalues.

**(v) Global order parameter.**

$$R_t^{(\omega)} \;=\; \frac{1}{n}\Big|\sum_{v=1}^{n} e^{i\phi_t^{(\omega)}(v)}\Big|, \qquad \overline{R^{(\omega)}} = \text{mean over the window.}$$

**A.3 Predictive mutual information (MI).** With render $\hat{s}_t$ and future projections $y_{t:t+\Delta}$:

$$\begin{aligned}
\text{(Linear–Gaussian)} \quad & \widetilde{\mathrm{MI}}_\Delta(\hat{s}_t; y_{t:t+\Delta}) \approx \tfrac{1}{2}\log\frac{\det\Sigma(y_{t:t+\Delta})}{\det\Sigma(y_{t:t+\Delta} \mid \hat{s}_t)}, \\
\text{(Nonlinear)} \quad & \widetilde{\mathrm{MI}}_\Delta(\hat{s}_t; y_{t:t+\Delta}) \approx \mathbb{E}\big[\log\hat{r}(\hat{s}_t, y_{t:t+\Delta})\big],
\end{aligned}$$

where $\hat{r}$ is a cross–validated density–ratio estimator (or use a $k$NN estimator; report $k$, metric, and bias correction).

**A.4 Counterfactual capacity surrogates.** **(i) Local attractor count.** Sample $M$ perturbations of radius $\kappa$ around $\hat{s}_t$; roll out $H$ steps under the closed loop; cluster endpoints into $\mathcal{A}_\kappa(\hat{s}_t)$; set $\mathcal{C} = \log|\mathcal{A}_\kappa(\hat{s}_t)|$.

**(ii) Controllability rank.** Estimate local Jacobian $J_f(\hat{s}_t)$ of the substrate/policy flow (finite differences or learned model); set $\mathcal{C} = \mathrm{rank}_\tau(J_f)$ with threshold $\tau$.

**(iii) Policy diversity.** For policy family $\Pi$, define $\mathcal{C} = \mathrm{Div}(\pi(\cdot \mid \hat{s}_t))$ (e.g., negative entropy or total variation distance to a prior).

**A.5 Null ensembles and standardization.** Let $x \in \{\widetilde{\mathrm{MI}}_\Delta, \mathcal{V}^{(\omega)}, \mathcal{C}, \widetilde{\mathrm{PE}}\}$ be a raw component. Generate $N$ surrogates per window from three classes and pool equally:

1. **Phase–scrambled:** randomize phase in the Fourier domain per channel and band, preserve amplitude spectrum.
2. **Time–shifted:** circularly shift each channel by a random lag $< T_{\mathrm{win}}$.
3. **Coupling–decoupled:** shuffle edges or attenuate off–diagonals in $S^{(\omega)}$ before forming $\mathbf{C}^{(\omega)}$.

Standardize via mixture z–score or quantile mapping:

$$\widetilde{x} = \frac{x - \mu_{\mathrm{null}}}{\sigma_{\mathrm{null}}} \quad \text{or} \quad \widetilde{x} = \mathrm{Q}^{-1}_{\mathrm{null}}(p_x) - \mathrm{Q}^{-1}_{\mathrm{null}}(0.5).$$

**A.6** TCI **definition (windowed).** For weights $(\alpha, \beta, \gamma, \delta) > 0$ and band weights $w_\omega$:

$$\mathrm{TCI}(t) = \alpha\, \widetilde{\widetilde{\mathrm{MI}}}_\Delta + \beta \sum_{\omega \in \Omega} w_\omega\, \widetilde{\mathcal{V}}^{(\omega)} + \gamma\, \widetilde{\mathcal{C}} - \delta\, \widetilde{\widetilde{\mathrm{PE}}}.$$

**A.7** TCI **computation (pseudocode).**

**(L1)** **Preprocess:** band–pass to $\Omega$, compute analytic signals, extract $a_t^{(\omega)}, \phi_t^{(\omega)}$.

**(L2)** **Coherence:** estimate $S^{(\omega)}$ (shrinkage $\rho$), form $\mathbf{C}^{(\omega)}$, compute $\mathcal{V}^{(\omega)} = \log\det(\mathbf{C}^{(\omega)} + \epsilon\mathbf{I})$ and $\overline{R^{(\omega)}}$.

**(L3)** **Render:** solve the TCNR inversion (few gradient steps on the render objective) to obtain $\hat{s}_t$; compute $\widetilde{\mathrm{PE}} = \|y_t - H_\Theta(\hat{s}_t)\|_2^2/m$.

**(L4)** **Predictive MI:** estimate $\widetilde{\mathrm{MI}}_\Delta(\hat{s}_t; y_{t:t+\Delta})$ (Gaussian closed form or nonlinear estimator).

**(L5)** **Counterfactuals:** evaluate $\mathcal{C}$ via the preregistered surrogate (attractor count / rank / policy diversity).

**(L6)** **Nulls:** generate $N$ surrogates from the three classes; recompute components on surrogates; obtain mixture $\mu_{\mathrm{null}}, \sigma_{\mathrm{null}}$ (or CDF).

**(L7)** **Standardize & combine:** produce $\widetilde{\cdot}$ and compute $\mathrm{TCI}(t)$ using the weights; store time series and per–band summaries.

**(L8)** **QC:** verify amplitude–vs–phase dissociation; save diagnostics (null overlays, eigenvalue spectra, MI calibration).

**A.8 Complexity notes (per window).** Coherence: $O(K\,n^2 T)$ to form $S^{(\omega)}$, $O(K\,n^3)$ for eigenvalues/log–det (use rank–$r$ for $O(K\,n^2 r)$). Nulls multiply cost by $N$. MI: closed form is $O(m^3)$; $k$NN is $O((m+d)\,W \log W)$ for $W$ samples and latent dim $d = \dim(\hat{s}_t)$. Real–time: prefer low–rank log–det updates (Cholesky) and one–step render descent with warm starts.

## B. Reporting Checklist (Bands, Windows, Nulls, Hyperparameters)

Use the following as a copy–paste section in Methods or Supplement.

- ☐ **Modalities and sampling:** modality, $f_s$, sensor geometry; re–referencing strategy.
- ☐ **Band set $\Omega$:** edges, transitions, filter design (order, zero/linear phase).
- ☐ **Windows & horizon:** $T_{\text{win}}$, step/overlap, prediction horizon $\Delta$; stationarity checks.
- ☐ **Coherence estimator:** multitaper/wavelet/Hilbert; shrinkage $\rho$; eigenvalue floor $\epsilon$; imaginary–coherence or spatial filtering used (Y/N).
- ☐ **Render details:** $H_\Theta$ class, optimization steps/step size, regularizers ($\lambda_\phi, \lambda_{\text{cf}}, \lambda_{\text{coh}}$); warm start policy.
- ☐ **Predictive MI:** estimator (Gaussian / density–ratio / $k$NN), hyperparameters, CV protocol.
- ☐ **Counterfactual surrogate:** (attractor count / rank / policy diversity), hyperparameters $(\kappa, H, \tau, M)$.
- ☐ **Null ensembles:** counts per class (phase–scrambled / time–shifted / decoupled), mixture rule, random seeds.
- ☐ **Weights:** $(\alpha, \beta, \gamma, \delta)$ after standardization; band weights $w_\omega$.
- ☐ **Statistics:** window–level rule (TCI$>0$), permutation scheme, CI method (block bootstrap), multiple–comparison handling.
- ☐ **Controls:** amplitude–only vs phase–only manipulations; decoupling; predeclared exclusion criteria.
- ☐ **QC artifacts:** null overlays, amplitude–phase dissociation plots, eigenvalue spectra, MI calibration on synthetic data.
- ☐ **Reproducibility:** commit hashes, environment (OS/versions), random seeds, hardware notes (GPU/CPU).

The section introduces a practical, preregisterable **decision procedure** for choosing the counterfactual-capacity term $e_C$ in the TCI. The user selects the surrogate based on experimental constraints and available models: (1) if a local closed-loop dynamical model around $\hat{s}_t$ exists (state-space or neural ODE), the preferred choice is the *controllability rank* $\text{rank}_\tau(J_f(\hat{s}_t))$; (2) if short closed-loop rollouts are computationally feasible, use the *local attractor count* $\log|A_\kappa(\hat{s}_t)|$ with a small radius $\kappa$, short horizon $H$, and clustering; (3) if only policies can be observed or sampled (without explicit dynamics), employ the *policy diversity* measure $\text{Div}_\pi(\cdot|\hat{s}_t)$, e.g., total-variation distance from a prior. Once chosen, this surrogate is preregistered. The section recommends an ablation analysis in which $e_C$ is omitted ($\gamma = 0$) and the resulting drop in behavior–TCI coupling (slope decrease, $p$-value increase) is reported, together with a small regression plot and mixed-effects summary. Reproducibility practices are emphasized: report runtime budgets and random seeds, log the exact hyperparameters $(\kappa, H, M)$ or $(\tau)$, publish the code commit, and provide null-standardized overlays to confirm that $e_C$ adds non-redundant variance beyond coherence and mutual information.

The appendices provide the technical underpinnings of the TCI pipeline. They define notation for band-limited analytic signals and describe coherence estimation via a shrinkage cross-spectrum $S^{(\omega)}$ and coherence matrix $C^{(\omega)} = D^{-1/2} S^{(\omega)} D^{-1/2}$, with an imaginary-coherence option for artifact robustness. The log-volume summary $V^{(\omega)} = \log\det(C^{(\omega)} + \epsilon I)$ can be approximated using the top $r$ eigenvalues, and a global order parameter $R^{(\omega)}$ quantifies phase synchrony. Predictive mutual information is estimated either in a linear-Gaussian form or using nonlinear

density-ratio or kNN estimators. Counterfactual surrogates are formalized as the attractor count, controllability rank, or policy diversity, while null ensembles mix phase-scrambled, time-shifted, and coupling-decoupled surrogates. Each component is standardized (mixture $z$-score or quantile mapping), and the windowed TCI is computed as

$$\mathrm{TCI}(t) = \alpha f_{\mathrm{MI},\Delta} + \beta \sum_{\omega} w_\omega e V^{(\omega)} + \gamma e C - \delta f_{\mathrm{PE}}.$$

Pseudocode (L1–L8) details preprocessing, coherence, render, MI, counterfactuals, null generation, and QC steps, while complexity notes discuss computational scaling and real-time optimization strategies. A reporting checklist specifies preregistration items: modality, bands, windows, nulls, hyperparameters, weights, statistical rules, controls, QC artifacts, and reproducibility metadata (commit hashes, environment, and seeds).

## Reporting and Transparency

This section summarizes the minimal information required for a fully transparent and reproducible TCI study. Researchers should complete each item in the checklist, substituting their own parameters and methods for the provided defaults. The goal is to make every component—from data collection to analysis and code provenance—explicitly verifiable.

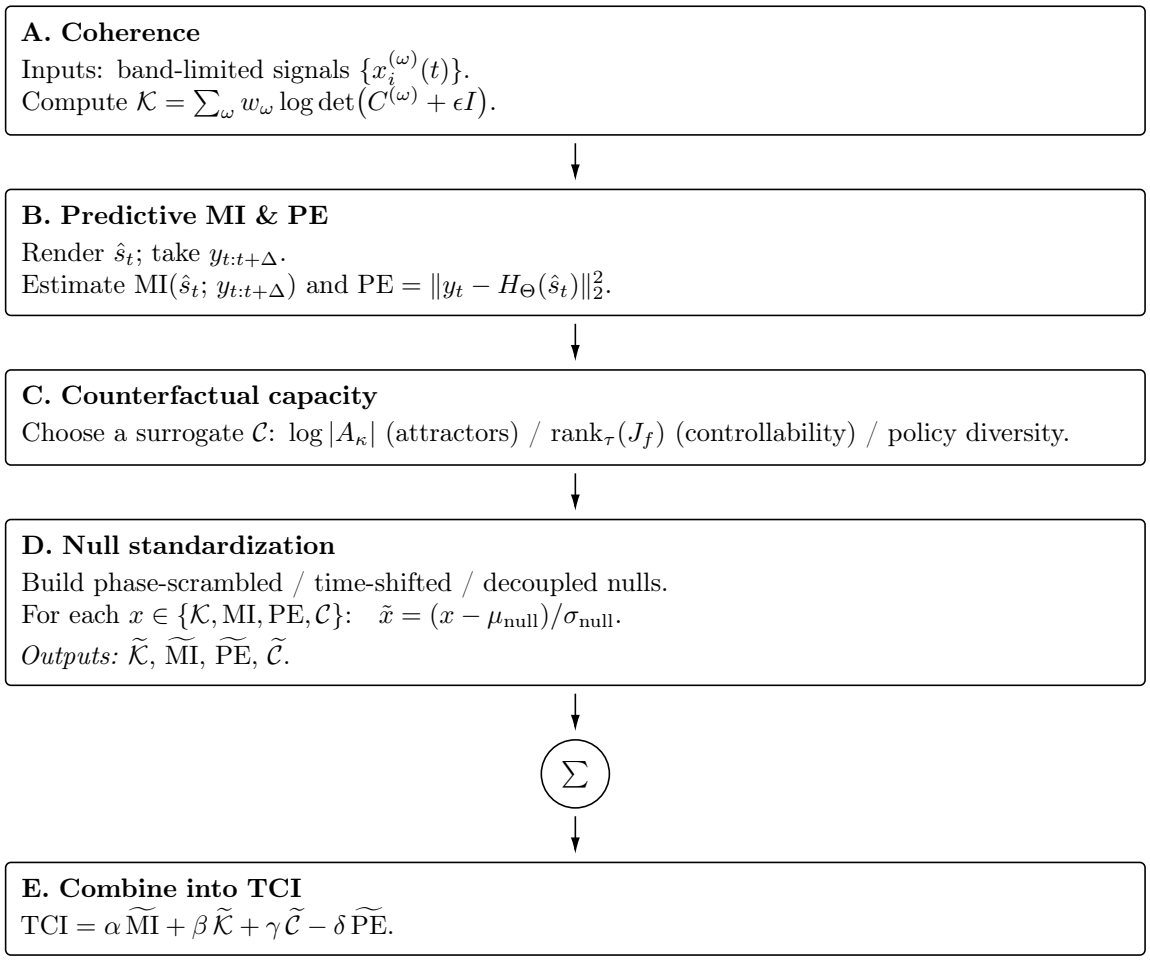


This figure shows how the Tomographic Consciousness Index (TCI) is built step by step. First, coherence (**A**) measures how well oscillations across different signals are synchronized. Next, predictive mutual information and prediction error (**B**) evaluate how much the current model state

predicts future data and how large the reconstruction error is. Then, counterfactual capacity (**C**) measures the system's ability to generate or explore alternative possibilities, estimated through one of three surrogates: local attractor count, controllability rank, or policy diversity. All these raw quantities are standardized in the null ensemble stage (**D**), where each measure is compared to its shuffled or surrogate baseline to isolate meaningful structure. Finally, the standardized components are combined in a weighted sum (**E**)—using weights $\alpha, \beta, \gamma, \delta$—to yield the overall TCI value, which represents the degree of coherence-based consciousness for that analysis window.

In plain terms, the pipeline formalizes how different informational and dynamical properties of a system contribute to conscious-like integration. It begins with raw signal structure (coherence and predictive coupling), then adds a measure of agency or flexibility (counterfactual capacity). By standardizing against randomized controls, it ensures that each feature contributes only its non-random, meaningful variance. The final weighted combination produces a single interpretable score of integrated predictive coherence—how well a system maintains coordinated, information-rich dynamics over time. This structure allows the same procedure to be applied consistently across very different substrates, from neural recordings to plant or artificial systems, providing a unified way to test and compare conscious processing.

## Tonic–Phasic–Ripple Motifs (Overview)

This section introduces three canonical signal motifs—*tonic carrier*, *phasic crossing*, and *fast ripples*—that recur across neural, plant, microbial, and engineered substrates. The figure provides a visual checklist for recognizing each pattern and for anticipating its effect on the TCI components: coherence (Coh), predictive information (MI), prediction error (PE), and counterfactual capacity (Ce). Tonic activity serves as a coherent timing scaffold (high Coh, little MI/PE change); phasic crossings produce event–locked bursts that typically raise MI and lower PE; fast ripples add fine predictive structure with modest MI/PE shifts. These motifs connect directly to the Six Conditions (Coh/Prop/Loop/Mem/Ag/Inf) and guide preregistration of analyses and perturbations in the methods that follow.

**Tonic (carrier)**

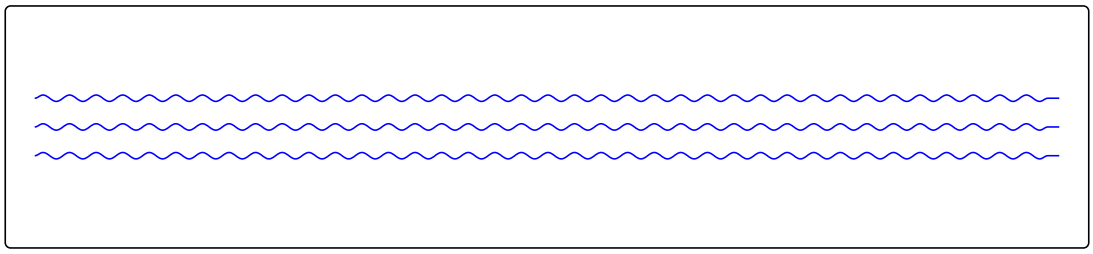

Coh: ↑ MI: ≈ PE: ≈ Ce: ≈ ⇒ TCI: small > 0

**Phasic crossing (burst on envelope)**

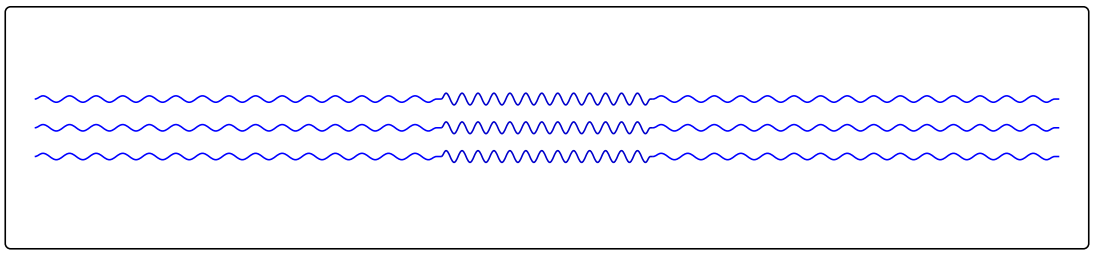

Coh: ∼ MI: ↑ PE: ↓ Ce: ↑ / ≈ ⇒ TCI: ↑

**Fast ripples on tonic**

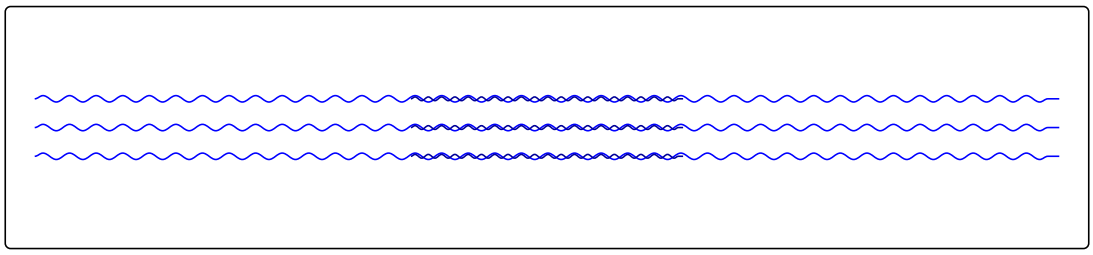

Coh: ≈ MI: ↑ (modest) PE: ↓ (slight) Ce: ≈ ⇒ TCI: ↑ (small)

**What the figure shows.** *Tonic (carrier).* Three channels share nearly the same phase and amplitude—useful as a timing scaffold but low in novel information. In TCNR terms: high coherence (Coh ↑), but no strong gains in predictive mutual information (MI ≈) or reductions in prediction error (PE ≈); counterfactual repertoire (Ce) is unchanged, so the net index (TCI) is only slightly above null.
*Phasic crossing (burst on envelope).* A brief segment exhibits higher amplitude and shorter period while riding the slow carrier. This is the classic cross-band phenomenon: a phase reset in the slow band that gates a fast burst (phase–amplitude coupling). The burst is informative about near-future projections, so MI ↑ and PE ↓. If the system can choose among alternative policies (nontrivial repertoire), Ce ↑; otherwise Ce ≈. Overall TCI increases.
*Fast ripples on tonic.* Small, high-frequency components are superimposed on the carrier without a large phase reset. Coherence changes little, but if the ripples systematically predict upcoming inputs (e.g., fine sensory detail or micro-control), MI increases modestly and PE falls slightly, nudging TCI upward.

**How to score these patterns (TCNR/TCI).** For each analysis window: (i) compute band-limited phases $\phi^{(\omega)}(t)$, global order $R^{(\omega)}(t)$, and coherence matrices $C^{(\omega)}(t)$; (ii) fit the

render model to obtain $\hat{s}_t$; (iii) estimate $\widetilde{\mathrm{MI}}(\hat{s}_t; y_{t:t+\Delta})$, the standardized log-det of $C^{(\omega)}$, a counterfactual surrogate $C_e$ (attractor count / controllability rank / policy diversity), and standardized prediction error $\widetilde{\mathrm{PE}}$; (iv) combine them as

$$\mathrm{TCI} = \alpha\,\widetilde{\mathrm{MI}} + \beta \sum_{\omega} w_\omega \log\det\big(C^{(\omega)} + \epsilon I\big) + \gamma\,\widetilde{\mathcal{C}} - \delta\,\widetilde{\mathrm{PE}}.$$

Tonic windows typically show high coherence but minor MI/PE movement; phasic windows show a transient MI increase and PE decrease; ripple windows show subtler changes.

**Predictions for plants (electrical / $\mathbf{Ca^{2+}}$).**

- *Tonic.* Circadian/ultradian carriers or slow-wave potentials yield Coh ↑, MI ≈, PE ≈.
- *Phasic crossing.* Wound, light, osmotic, or hydraulic shocks produce event-locked phase resets in slow bands with fast $Ca^{2+}$ bursts nested on the envelope: PAC ↑, MI ↑, PE ↓, TCI ↑.
- *Ripples.* Fine, fast components during active foraging/growth control: modest PAC/PPC signatures; small MI gains.

**Ultrafast/"quantum" note (photosynthetic complexes).** At femto–picosecond scales, vibronic/excitonic coherences produce beat-like mixing (short-lived, local). This is analogous to the phasic/ripple idea (frequency mixing), but *not* a tissue-scale traveling wave. Expect strong coherence locally with rapid decoherence; the TCNR pipeline applies if instrumentation can feed those projections to a render model (e.g., pump–probe sequences mapped to $\hat{s}_t$) and metrics are standardized to appropriate nulls.

**How to falsify.** (1) *Amplitude-only* manipulations should leave MI and PE essentially unchanged while apparent coherence remains high. (2) *Phase decorrelation* should reduce MI and raise PE even if power is intact. (3) *Decoupling* (e.g., blocking inter-site coupling) should collapse directionality measures (phase-gradient transport) and drop TCI.

**Mapping to the Six Conditions.** Tonic satisfies **Coh** and **Prop** but not **Loop**/**Mem**/**Ag**/**Inf**; phasic crossing temporarily satisfies **Loop** and **Inf** (sometimes **Ag**); ripples contribute to **Inf** with minimal change to **Coh**. Conscious-adequate windows require all six to register above preregistered thresholds; the figure illustrates how different signal motifs push the components. [13]

[13] **Companion relationship.** This paper is one of a two-part study comprising: (i) *Tomographic Coherence–based Neural Rendering (TCNR): Formalism, a Cross–Substrate Consciousness Index, and Falsifiable Tests* (Blumberg, 2025), which develops the empirical and computational framework for coherence–based rendering and defines the Tomographic Consciousness Index (TCI); and (ii) *The Necessary Mind from Coherence: A Computational Proof of God* (Blumberg, 2025), which extends the TCNR mechanism into a formal metaphysical proof using the Principle of Sufficient Reason (PSR) and modal logic S5. Together the two papers form a closed empirical–philosophical loop: TCNR provides the mechanistic and mathematical foundation, while the Proof of God formalizes its logical and ontological implications.